LBNL-50863

Comparative Dosimetric Estimates of a 25 keV Electron Microbeam with Three Monte Carlo Codes

Enrico Mainardi, Richard J. Donahue, Eleanor A. Blakely

Keywords

Electrons and Photons transport, Monte Carlo Codes, Electron micro-beam, Microdosimetry

September 2002

Abstract

Comparative Dosimetric Estimates of a 25 keV Electron Microbeam with Three Monte Carlo Codes

by

Enrico Mainardi, Richard J. Donahue, Eleanor A. Blakely

The calculations presented compare the different performances of the three Monte Carlo codes: PENetration and Energy LOss of Positrons and Electrons code (PENELOPE-1999), Monte Carlo N-Particle transport code system (MCNP-4C), Positive Ion Track Structure code (PITS), used for the evaluation of dose profiles from a 25 keV electron micro-beam traversing individual cells. The overall model of a cell is a water cylinder equivalent for the three codes but with a different internal scoring geometry: water filled cylindrical shells for PENELOPE and MCNP, whereas spheres are used for the PITS code. A cylindrical cell geometry with scoring volumes with the shape of water filled cylindrical shells was initially selected for PENELOPE and MCNP because of its superior simulation of the actual shape and dimensions of a cell and for its improved computer-time efficiency if compared to spherical internal volumes. Some of the transfer points and energy transfer that constitute a radiation track may actually fall in the space between spheres, that would be outside the spherical scoring volume. This internal geometry, along with the PENELOPE algorithm and along with the combination of numerical and analytical differential cross sections, drastically reduced the computer time when using this code if comparing with event-by-event Monte Carlo codes like PITS.

This preliminary work has been important to address dosimetric estimates at low electron energies. It demonstrates that codes like PENELOPE can be used for dose evaluation, even with such small geometries and energies involved, which are far below the normal use for which the code was created. Further work (initiated in Summer 2002) is still needed, to create a user-code for PENELOPE that allows uniform comparison of exact cell geometries, integral volumes and also microdosimetric scoring quantities, a field where track-structure codes like PITS, written for this purpose, are believed to be superior.

Table of Contents

List of Figures

List of Tables

REPORT #: **LBNL-50863**

EnricoEnrico Mainardi; Richard J. Donahue; Eleanor A. Blakely

Comparative Dosimetric Estimates of a 25 keV Electron Microbeam with Three Monte Carlo Codes

Abstract

The calculations presented compare the different performances of the three Monte Carlo codes: PENetration and Energy LOss of Positrons and Electrons code (PENELOPE-1999), Monte Carlo N-Particle transport code system (MCNP-4C), Positive Ion Track Structure code (PITS), used for the evaluation of dose profiles from a 25 keV electron micro-beam traversing individual cells. The overall model of a cell is a water cylinder equivalent for the three codes but with a different internal scoring geometry: water filled cylindrical shells for PENELOPE and MCNP, whereas spheres are used for the PITS code. A cylindrical cell geometry with scoring volumes with the shape of water filled cylindrical shells was initially selected for PENELOPE and MCNP because of its superior simulation of the actual shape and dimensions of a cell and for its improved computer-time efficiency if compared to spherical internal volumes. Some of the transfer points and energy transfer that constitute a radiation track may actually fall in the space between spheres, that would be outside the spherical scoring volume. This internal geometry, along with the PENELOPE algorithm and along with the combination of numerical and analytical differential cross sections, drastically reduced the computer time when using this code if comparing with event-by-event Monte Carlo codes like PITS.

This preliminary work has been important to address dosimetric estimates at low electron energies. It demonstrates that codes like PENELOPE can be used for dose evaluation, even with such small geometries and energies involved, which are far below the normal use for which the code was created. Further work (initiated in Summer 2002) is still needed, to create a user-code for PENELOPE that allows uniform comparison of exact cell geometries, integral volumes and also microdosimetric scoring quantities, a field where track-structure codes like PITS, written for this purpose, are believed to be superior.

General Introduction

This report summarizes the results of comparative Monte Carlo simulation work of the energy deposition of a 25 keV electron microbeam in water. [1] The main result of the calculations presented here is a comparison of the total energy deposited within a biological cell system by a 25 keV electron micro-beam, calculated by three different Monte Carlo Computer Codes: PENetration and Energy LOss of Positrons and Electrons code (PENELOPE-1999), Monte Carlo N-Particle transport code system (MCNP-4C), Positive Ion Track Structure code (PITS). This analysis provided preliminary work for further studies planned for lower energy photon sources. The computational work reported here was designed to support experiments in progress at the LBNL Advanced Light Source (ALS), and for the interpretation of their results. In addition, the comparative Monte Carlo analyses completed are important to benchmark with real experiments the performance of current computer codes which have not been tested at energies less than 25 keV. In particular there is research planned to use a 12.5 keV x-ray micro-beam at the ALS to irradiate human mammary epithelial cells and fibroblasts to investigate bystander effects of low doses of radiation in unirradiated cells neighboring irradiated cell cohorts, with funding support from the Department of Energy's OBER Low-Dose Radiation Program.

[1] The work was completed by Enrico Mainardi at the Lawrence Berkeley National Laboratory (LBNL) during the Summers of 2001 and 2002. Enrico Mainardi was a visiting PhD student from the University of Rome "La Sapienza", under the direct supervision of Dr. Richard Donahue of the Environment, Health & Safety (EH&S) Division of LBNL and Dr. Eleanor Blakely of the Life Sciences (LS) Division of LBNL, and with the external and fundamental co-operation of Dr. Walter Wilson of Washington State University at Richland (WSU).

This report focused on the comparison of energy deposition calculations in a cell of 10 μm in radius and 10 μm thick irradiated with a 25 keV electron microbeam. The calculations were performed with the computer codes PENELOPE, MCNP, PITS. The energy deposition modeling results presented in the paper by Wilson et al. [2] were the starting point of our comparison and collaboration with him. Although the 25 keV electron source is different from the 12.5 keV x-rays source the nature of the problem is similar because the evaluation of the electron transport has an essential and relevant part for both problems and this report represents the starting point for the next computational work on this second source type. A 12.5 keV photon passing through the cell will produce photoelectrons with subsequent secondary production and transport of electrons; before they can be absorbed they continue to produce electrons and electron showers. Both PENELOPE and MCNP codes transport both electrons and photons in different materials, while modules added to the PITS code provide the capability to transport photons and simulate their transport through other material media in addition to water.

The first part (PART I) of this report includes a brief introduction to the most common terminology in the field of microdosimetry and of Monte Carlo electron and photon transport. This part will be illustrative only, rather than exhaustive, and includes a list of some Monte Carlo codes used for general and biological problems and their energy cutoff. Some of these codes were considered initially, but later the focus shifted to PENELOPE, MCNP, PITS because of their availability and applicability to the problem involving small scale dimensions (of the order of 10μm), and transport of small energy electron-photon (source of the order of 10-30keV). This first part also includes a description of the rationale for our focus on computer simulations of biological problems and interpretation of their experimental results, in particular addressing DOE interests.

In the second part (PART II) of the report there are some results from simulations performed on a PC and UNIX workstation employing PENELOPE [c1] and MCNP 4C [c2]: two general purpose Monte Carlo codes that also track photons and electrons. The main purpose of this section is the comparison of these two general purpose Monte Carlo codes against published results from the Monte Carlo track code PITS [c3, c4], to test their applicability for dose profiles evaluation and for microdosimetry problems. The relevant quantity used for this initial comparison is the dose, which is a macroscopic quantity, but tallied for a problem in the microscopic space scale and for energies lower than the one used normally for macroscopic problems.

Finally, the report draws conclusions from, and explains the limitations of this preliminary work, which was necessary in the learning process towards a more detailed microscopic code development. In order to be able to use macroscopic codes such as PENELOPE and MCNP, some modifications to the codes themselves needed to be done in order to score microscopic quantities in an appropriate way. In particular PENELOPE proved to have better results for dose radial profiles, and demonstrated a better applicability to future microdosimetric problems. Future work will concentrate on the development of more specific user-codes in order to consider geometry specification common to the microdosimetric field (subdivided into spheres) and the tally of particular quantities (e.g., frequency-mean specific energy, lineal energy, energy imparted, event frequency spectra) that are related to macroscopic quantities but cannot be drawn directly from them without further simulation development.

PART I

Computer simulations for biological problems

Bystander effect of radiation involves the study of the biological response of cells that are not directly traversed by radiation, but are neighbors of irradiated cells. Bystander cells have been shown to respond in a number of ways: with gene induction and/or the production of potential genetic and carcinogenic changes. The mechanisms underlying bystander effects of low-LET (linear energy transfer) radiations delivered at low total doses or dose-rates are unknown [c11, c12]. Such effects could potentially increase the estimates of risk from low dose radiation.

Energetic electrons from low-LET x- or γ-ray exposures traverse many cells before they stop. Multiple scattering generates subsequent photoelectric effects and a broadening of the energy deposition field. Collimated micro-beams of electrons offer an approach that may allow a more accurate determination of the radiation dose and bystander effects at low doses of low LET radiation. Few Monte Carlo codes however extend down to the energy range of the electron micro-beams. This manuscript is focused on the goal of estimating dosimetric values for low energy electron $\leq$ 25 keV micro-beams.

Macroscopic and Microdosimetric calculations

Microdosimetry is defined as the study of energy deposition processes in biological media with particular emphasis on phenomena correlated with the physical aspects of the radiation action on living systems. Important quantities defined in microdosimetry and fully described in ICRU REPORT 36 [1] are: *energy imparted* $\mathbf{E_n}$, *specific energy* **Z**, *lineal energy* **Y**.

The *energy imparted* $\mathbf{E_n}$ to the matter in a volume (scoring volume) is

$\boldsymbol{E_n = \Sigma_i (E_{ni}) = \Sigma_i (T_i - T_{out} + Q_{\Delta m})_i}$ where

E_n = summation performed over all energy deposits E_{ni} expressed in terms of joule (J) or eV

T_{in} = energy of the incident ionizing particle

T_{out} = sum of the energies of all ionizing particles leaving the interaction

$Q_{\Delta m}$ = changes of the rest mass energy of the atom and all particles involved in the interaction

The *specific energy* **Z** is the energy imparted by ionizing radiation to matter of a scoring volume of mass *m* and it is expressed in terms of joule per kilogram (J kg^{-1}) or Gy (1 Gy = 1 J kg^{-1}): $\boldsymbol{Z = E_n/m}$.

The *lineal energy* **Y** is the energy imparted to matter in a volume by a single energy-deposit event divided by the mean cord length *l* in that volume and it is expressed in terms of joule per meter (J m^{-1}) or in keV μm^{-1}: $\boldsymbol{Y = E_n/l}$.

In this preliminary work only the macroscopic quantity *dose* **D** is computed and presented and expressed in terms of (Gy) and also in (keV/μm^3), considering the density to be 1 g cm^{-3}.

The scoring volumes defined for the PENELOPE and MCNP models (water filled cylindrical shells) did not allow the use of the mean cord length *l* definition that is applicable for the PITS model (spherical scoring volumes). Also other microdosimetric quantities were not computed. Nevertheless the results of the PITS code included the macroscopic quantity *dose* **D** calculated in each sphere in order to define a radial and penetration profile. The dose distributions were obtained from the specific energy **Z** distributions multiplying the value of **Z** in each sphere by the probability of that sphere being hit by radiation $P_{hit\text{-}i}$: $D_i = Z_i \bullet P_{hit\text{-}i}$.

A *transfer point* **T(x,y,z)** refers to the geometric position of radiation interactions while the energy deposited locally at this point is also called the *energy transfer*. The *Linear Energy Transfer* is the energy deposited locally, in the form of excitation or ionization, per unit path of a charged particle. The physical description of an ionizing particle is complete when all transfer points and energy transfers are known, and listing of this data constitutes a *radiation track*. The shape of a radiation track is formed by multiple ionizations, excitations, and elastic scattering events and is highly structured and stochastic.

There are two fundamental mechanisms by which radiation can affect biological cells. One may lead to the breakage of molecules, rupturing their bonds by the ionizing effect of the radiation (direct effect). The second mechanism, again because of excitation, may result in the production of new chemicals, such as the highly reactive oxy (O) and hydroxyl (OH) radicals, which interact chemically within the cell, producing the more important biological effects (indirect effect). The effect of high-LET radiation is greater than low-LET radiation per absorbed dose.

Low-LET radiations produce a non-uniform spectrum of secondary electrons, which are scattered in space and energy. Most of the energy deposited is in the form of sparsely distributed

ionizations and excitations. However, as the primary particle loses energy, the increased interaction cross section leads to a higher density of events.

On the contrary, high-ionization densities characterize high-LET radiations. At the cellular level non-uniformities in energy deposition are much greater for high LET events than for low-LET events. For a given dose approximately the same number of ionizations and excitations will occur for both low- and high-LET events; however, the high-LET events will be more concentrated in space. When compared to the low-LET radiations, the tracks of high-LET radiations are very localized at the scale of the cell nucleus. Due to the greater mass of high-LET particles, ejected secondary electrons have small energies and shorter ranges. A high-LET particle will deposit its energy densely in a small number of targets, even including δ-ray effects. In contrast, low-LET hits are sparsely distributed and characterized by low-energy transfers.

Monte Carlo codes for photons and electrons transport

A 3-D transport calculation of the radiation penetrating through a cell and what scatters out toward neighboring cells and that takes into account the complexity of the system, requires Monte Carlo methods. The development of efficient and precise models for geometric, source and material representation and analysis is necessary. The answers for the different zones of a cell system include:

D(r) = total mean values of dose in zones of a cell by photons (P) and electrons (E) and normalized by the volume of the zones as function of radial distance (r). Expressed in both (Gy) and (keV/μm^3)

D(x) =mean values of energy deposited in zones of a cell by photons (P) and electrons (E) and normalized by the volume of the zones as function of penetration (x). Expressed in both (Gy) and (keV/μm^3)

D(x,r) =3-D plot of dose distributions as function of penetration (x) and radial distance (r). Expressed in both (Gy) and (keV/μm^3)

T(x,y,z) =3-D plot of the electrons' tracks inside the cell obtained connecting transfer points

This work is important to evaluate the performance of general-purpose Monte Carlo codes like PENELOPE and MCNP compared to Monte Carlo event-by-event codes like PITS for microdosimetric applications underlining their main difference in computational approach and results.

The transport of electrons through a liquid water homogeneous medium has been simulated using Monte Carlo transport methodology. The essence of Monte Carlo consists of simulating particle histories using a pseudo-random number generator used to sample probability distributions for particle events (such as, scattering angles, energy transfer, collisions etc.) using cross-sectional data describing such events. Because Monte Carlo methods rely on the result of stochastic events to continue the history, most practical three-dimensional geometries may be modeled easily. Because Monte Carlo tallies are dependent on events occurring within the region of interest, regions in which few events occur yield a statistically poor answer unless a large number of particle histories are run.

The transport of electrons is dominated by the long-range Coulomb force, resulting in a large number of small interactions that cause a great increase in computational complexity. Traditional Monte Carlo codes are widely used to calculate macroscopic phenomenon (such as, absorbed dose, flux etc.). Normally, to reduce computing time these codes compute electron events based on condensed histories. A condensed history groups several discrete events together into one event thus reducing the total number of events in the track history. For macroscopic calculations this technique gives good results; however, at the microscopic level this calculation may provide insufficient information on the nature of the particle history. In addition, most practical codes have a lower energy electron cutoff between 1 and 10 keV thus it is believed that they are insufficient tools for stochastic applications in micro-scale geometries.

Among many other Monte Carlo codes, two standard macroscopic codes: PENELOPE [c1] and MCNP [c2] were selected and used for our problem. We expected reasonable results despite the small sizes and energies involved that could have been a problem for general-purpose codes designed for other applications and not specifically for this microdosimetry field where track-structure codes are superior. Some other major codes for the simulation of electrons and other particles in different energy range and for different purposes are listed here for reference: TART97 [c5], EGS4 [c6, c7], ETRAN [c8, c9], ITS [c10, c11], TIGER [c12], PTRAN [c13] and presented in Table1. Macroscopic programs mainly use condensed history techniques based on analytic and semi-analytic multiple scattering theories such as the one of Moliere and Goudsmit-Saunderson to transport electrons down to values generally not smaller than 1 keV. The multiple scattering theories implemented in condensed simulation algorithms are only approximate and may lead to systematic errors. The multiple-elastic scattering theory of Moliere (1948), which is the one used in EGS4-based codes, is not applicable to step lengths shorter than a few times the elastic mean free path. In the next paragraph the algorithm and scattering model used for MCNP and PENELOPE is presented. In general condensed schemes also

have difficulties in generating particle tracks in the vicinity of an interface (i.e. a surface separating two media of different compositions). When the particle moves near an interface, the step length must be kept smaller than the minimum distance to the interface, so as to make sure that the step is completely contained in the initial medium (this is not our case since the material is water).

Electron-track codes are very different than commercially available, macroscopic programs and microdosimetry has benefited greatly from the development of these codes that can simulate event-by-event electron interactions (not in a condensed way) down to very low energies. Table1 gives references and general information for some published electron track codes used in microdosimetry and radiobiology; these are PITS [c3, c4], MOCA8b [c14, c14b] , MOCA14 [c15], OREC [c16, c17], CPA100 [c18, c19], DELTA [c20], ETRACK [c21, c22], KURBUC [c23], TRION [c24], ESLOW [c25]. Almost all the track structure codes use cross sections based on water in either the vapor or liquid phase. In fact, the classification of an electron track code is based on the phase, condensed or vapor, of the water cross sections. All vapor phase codes scale the density of the water vapor to 1 g/cm^3 as an approximation of liquid water. Reference [5] by Nikjoo summarizes the structure and comparative performance of two liquid and two vapor phase track structure codes. The general agreement between the predominant track codes is quite good for calculations of radial interaction frequencies and radial energy depositions. However, calculations predicting spatial distributions and energy depositions in nanoscale targets show considerable disagreement [5]. The work of Stewart et al. [9], to examine the microdosimetric properties in water using a test of the PENELOPE code system indicates that PENELOPE may prove particularly useful for applications that involve radiation transport through materials other than water or for applications that are too computationally intensive for event-by-event Monte Carlo, such as in vivo microdosimetry of spatially complex distributions of radioisotopes inside the human body. These authors stated that to their knowledge, PENELOPE is the first widely available, general purpose Monte Carlo code system capable of transporting electrons and positrons in arbitrary media down to such low energies which opens the possibility of using it for microdosimetry.

There are roughly 10 track structure research codes, prevalent in the literature (Table 1) while there are numerous general purpose Monte Carlo codes for radiation transport although only few are indicated in Table 1. These Monte Carlo codes may differ in the following ways:

1. ***Cross section data*** (e.g. number of elements that the code can deal with, way they are used, their origin);

2. ***Physical interpretation and assumptions*** (e.g. physics of photon interactions, physics of electron transport, energy cutoff, treatments of Auger electron emission, characteristic x-ray emission);

3. ***Monte Carlo methodology*** (e.g. event-by-event or condensed history techniques, probability distribution functions, random number generation, and sampling techniques).

Of these topics, the most predominant factor affecting the output of the code is the differences in cross section data. Also very important are the physical assumptions used in determining the mechanics of the electron transport.

CODE	Particles	Reference	WEB SITE
MACROSCOPIC CODES:			
PENELOPE	P, E;	c1	http://www.nea.fr/abs/html/nea-1525.html
MCNP	N, P, E;	c2	http://laws.lanl.gov/XCI/PROJECTS/MCNP/
TART	N, P;	c5	http://www.nea.fr/abs/html/ccc-0638.html
EGS4	P, E, I;	c6, c7	http://www.nea.fr/abs/html/ccc-0331.html http://ehssun.lbl.gov/egs/egs.html
ETRAN	P, E, I;	c8, c9	http://www.nea.fr/abs/html/ccc-0107.html
ITS	P,E;	c10, c11	http://www.nea.fr/abs/html/ccc-0467.html
TIGER	P, E;	c12	
TRACK CODES:			
PITS	P,E,I;	c3, c4	http://www.tricity.wsu.edu/~wwilson/pits.html
PTRAN	P;	c13	
MOCA8	P, E;	c14, c14b	
MOCA14	P, E;	c15	
OREC	P, E;	c16, c17	
CPA100	P, E;	c18, c19	
DELTA	P, E;	c20	
ETRACK	E;	c21, c22	
KURBUC	P, E;	c23	
TRION	P, E;	c24	
ESLOW	P,E,I;	c25	http://www-xdiv.lanl.gov/XTM/tme/cv.html

Table1: General information and references for published Monte Carlo track codes and some general-purpose codes.

PENELOPE and MCNP vs. PITS

This section reports preliminary work needed to evaluate the performance of general-purpose Monte Carlo codes like PENELOPE and MCNP, compared to Monte Carlo Track-structure codes like PITS in the microdosimetric field. The main advantage of using a general-purpose Monte Carlo code is its easier availability and the fact that normally it's more user-friendly, especially if compared with a Monte Carlo track-structure code created *ad hoc* for a certain problem related to the tracking of photon or electrons by a specific group or by a single researcher. Most important an advantage might be the possibility to have answers for many materials other than water, that can affect the calculations. Also, general codes are more widespread and available to more people from which suggestions and "bug discovery" can be revealed. They are subject to more frequent up-grades and benchmark from the authors and from the users, and due to the interaction of both.

In this paragraph we outline the main differences of the three codes regarding the characteristic mentioned in the previous paragraph:

1. Cross section data;
2. Physical interpretation;
3. Monte Carlo methodology.

1. Cross section data include the number of elements that the code can deal with, the way they are used and the origin of these data. To meet the possibility to use the code in all situations, general-purpose Monte Carlo codes have the possibility to deal with all elements or most of them, while track codes are in general designed to deal with a limited number of elements or only water. Of course microscopic codes can also deal with more materials, and can be extended in applicability to other fields but only after some work.

PITS, as for most existing Monte Carlo codes, is for water vapor adjusted to density of 1 g cm^{-1} and does not include the elemental composition of tissue. Interaction cross sections are known to be different for liquid water but they are less well-established and less open to experimental measurements.

In MCNP there are two electron interaction data libraries (el03 and el01) that contain data on an element-by-element basis for atomic numbers Z=1-94.

PENELOPE combines numerical total cross sections (or stopping cross sections) with simple analytical differential cross sections. Using analytical formulas to get cross sections data contributed to speed up the calculations.

2. Physical interpretation. All the codes used in this comparison simulate in a detailed way the common photon interactions: Photoelectric effect, Rayleigh scattering, Compton scattering and electron-positron pair production.

PITS tracks electrons down to 10 eV. It can simulate the interactions of low energy photons, such as the characteristic x-rays of Carbon (278 eV), Aluminum (1487 eV) and Titanium (4509 eV). The three important interactions, photoelectric effect, coherent (Rayleigh) scattering, and incoherent (Compton) scattering are included. The photo effect, since it is the more frequent, is simulated by "table-lookup". The other two interactions are simulated via the Monte Carlo rejection method using Klein-Nishina theory and published form factors and scattering functions. Bremsstrahlung production, fluorescence photons and beam focusing are features yet to be included. [c3, c4]

MCNP-4C covers both photon and electron energies from 1 keV. Auger electrons are modeled crudely, and for example L-shell fluorescence is not implemented. For the applications presented in this paper these shortcomings may be irrelevant. [c2 pag. 2-74]

PENELOPE covers photon energies in the range from 1 keV to 1 GeV, and electron energies from 100 eV to 1 GeV. [c1]

3. Monte Carlo methodology.

Codes like PITS deal with event-by-event simulations using a detailed-history Monte Carlo method and track electrons down to 10 eV. In particular calculations were performed with the delta-ray transport module of the PITS set of radiation simulation codes. The delta-ray source-term energy was set to the desired mono-energetic beta-ray energy (25 keV). The delta-ray transport module is an event-by-event, detailed-histories Monte Carlo simulation of non-relativistic electron slowing down in unit-density water, based on measured cross-sections for electron scattering from water molecules. [c3, c4]

MCNP uses a condensed history techniques based on the multiple-scattering theory of Goudsmit-Saunderson for angular deflections, the Landau theory of energy-loss fluctuations and the Blunck-Leisegang enhancements of the Landau theory. These theories rely on a variety of approximations, and don't solve the entire transport problem. In particular, it is assumed that the energy loss is small compared to the kinetic energy of the electron. In order to follow an electron through a significant energy loss, it is necessary to break the electron's path into many steps. These steps are chosen to be long enough to encompass many collisions (so that multiple-scattering theories are valid) but short enough that the mean energy loss in any one step is small (so that the approximations necessary for the multiple-scattering theories are satisfied). The energy loss and angular deflection of the electron during each of the steps can then be sampled from probability distributions based on the appropriate multiple scattering theories. This collection of the effects of many individual collisions into single steps that are sampled probabilistically constitutes the "condensed history" Monte Carlo method.

The electron physics in MCNP is essentially that of the Integrated TIGER Series [c12], which is based on the condensed history method of the ETRAN series of electron/photon transport codes [c8, c9]. With MCNP-4C the MCNP *F8 tally has been used in order to calculate the energy deposited in a cell. The *F8 tally is the difference between the energy carried into and out of the cell by particles. Dividing the net energy deposited in the cell by the mass of the cell, the *average dose in the cell (called D and measured in Gy)* is, by definition, obtained. If one divides large cell (cylinders of 10μm radius and height) into tally segments (spheres of 1μm diameter) these become small compared to the major steps and sub-steps that the code uses for the condensed-history transport of electrons. In such a case the results in the cell may be wrong and even the macroscopic transport may be affected. The problem originates from the fact that electron tracks are interrupted at cell boundaries and certain approximations are made for crossing these boundaries. For these smaller geometries it was necessary to introduce a factor (ESTEP) to reduce the length of electron sub-step. [c2 pag.2-63, 3-108]

PENELOPE on the other hand uses an algorithm that incorporates a scattering model that combines numerical total cross sections (or stopping cross sections) with simple analytical differential cross sections for the different interaction mechanisms. Individual interaction events are simulated by means of purely analytical, exact sampling methods, so that the structure of the simulation code is very simple. For electron transport PENELOPE implements a "mixed" simulation scheme, which combines the detailed simulation of hard events where the value of the scattering angle and energy loss are large

(i.e. events with polar scattering angle O or energy loss W larger than previously selected cutoff values Os and Wc) with condensed simulation of soft events (i.e. in which O<Os or W<Wc).

With PENELOPE it is necessary to adjust to the small geometries (if compared with macroscopic problems) varying the value of DSMAX that defines the maximum allowed electron step length. When the particle moves in a thin body like the cell of our case the DSMAX was given a value of the order of one tenth of the 'thickness' of that body (0.1μm= 1/10 of layer thickness). Normally (as Default), for relatively thick bodies (e.g. thicker than 10 times the mean free path between hard interactions), the step length control is switched off by setting DSMAX to a large value (DSMAX=$1.0 \bullet 10^{35}$).

PART II

Setup with the 3 codes

The geometrical model in the Monte Carlo simulations is a cylinder centered on the z-axis as presented in Figures 1.1 and 1.2 with both Radial and Vertical view. The cylindrical volume is 9μm deep with a radius of 10μm made of water; this would allow a direct comparison with the results of the PITS code [2].

The cylinder has 9 layers (defined by XY planes), each 1μm height for a total cylinder thickness of 9μm. Inside the cylinder with outer radius R_{out} of 10μm there are several other cylinders with the same Z axis and thickness of 9μm but with different diameters that define the zones or scoring volumes of the cell. Since the sizes of the zones of the cell are different, in order to obtain the dose profiles, it is necessary to normalize the energy deposited in each zone dividing it by its volume or mass as explained later in the following sections.

This cylindrical geometry was considered a good model for a generic cell and it is very useful to score depth and radial profiles for dose, from a pencil beam. Such geometry is also essential to compare PENELOPE and MCNP result with those obtained with the track code PITS.

The source is a 25 keV electron micro-beam pointing, along the z-axis, toward the cylinder.

Several cases and models –listed in Table2- were studied in order to learn and to evaluate the performance of the PENELOPE and MCNP codes especially comparing it to the PITS code. Only the more significant cases are explained in more details and their results plotted.

Two FORTRAN user-codes, called PENRICO and PEN (PEN is an improved version of PENRICO), were created starting from modification of PENLAYER, an example included in the PENELOPE code package. The creation of the user-codes PENRICO and PEN is essential in order to model and adapt the geometry, the material, the source and tallies to the case of interest for this comparison. Each of the user-codes had to be linked with the main PENELOPE code. Some of the parameters can than be changed through an INPUT file for each of the user-codes. Different simulation parameters were changed in order to study the code and its responses using different INPUT files.

The MCNP model was made identical to the PENELOPE one. Also with MCNP different simulation parameters and material data libraries were used, modifying and using different MCNP INPUT files.

The PITS geometrical scoring volume model is slightly different from the one described although the set of results data provided courtesy of the author (Walt Wilson) can be compared to the one from the PENELOPE and MCNP codes. In PITS the Energy Deposited is evaluated inside spheres of 0.5μm radius (scoring volumes) within the cylindrical volume that has 10μm radius and 9μm deep.

In conclusion the simulation geometrical model is essentially the same for all three codes although PITS uses a different spherical scoring geometry internal of the cell instead of water filled cylindrical shells used for the other codes. An important advantage of cylindrical cell geometry with scoring volumes with the shape of water filled cylindrical shells is its improved "computer-time efficiency" if compared to spherical internal volumes. This is because some of the transfer points and energy transfer that constitute a radiation track may actually fall in the space between spheres, so outside the spherical scoring volume. Of course for a very large amount of histories (or tracks) computed this would not affect the results. The disadvantage of such geometrical scoring volumes is their bigger size, compared to the spherical zones used for PITS, especially for large values of the outer radius R_{out}; this would allow an "easier" comparison and doesn't require the detailed information of the spherical model, which is normally used to score microdosimetric quantities.

CASE NAME	ENERGY CUTOFF	DSMAX	COMPUTER TIME	DIMENSIONS
PENRICO2.IN	100eV	DSMAX=MAX	10min=600 sec	**Radius=1um; Total Thickness=10um**
PENRICO3.IN	100eV	DSMAX=MAX	11min=660 sec	Radius=10um; Total Thickness=10um
PENRICO4.IN	100eV	DSMAX=MAX	11min=660 sec	**Radius=10um; Total Thickness=9um**
PENRICO5.IN	100eV	DSMAX=MAX	11min=660 sec	**Radius=10um; Total Thickness=4.5um**
PENRICO8.IN	100eV	DSMAX=MAX	21.5min=1290 sec	Radius=10um; Total Thickness=9um
PENRICO9.IN	100eV	DSMAX=MAX	21hr=75600 sec	Radius=10um; Total Thickness=9um
PENRICO10.IN	1keV	DSMAX=MAX	60min=3600 sec	Radius=10um; Total Thickness=9um
PENRICO11.IN	1keV	DSMAX=MAX	60min=3600 sec	Radius=10um; Total Thickness=9um
PEN01.IN	1keV	DSMAX=0.1	10min=600 sec	Radius=10um; Total Thickness=9um
PEN02.IN	1keV	DSMAX=0.1	30min=1800 sec	Radius=10um; Total Thickness=9um
PEN03.IN	100eV	DSMAX=0.1	60min=3600 sec	Radius=10um; Total Thickness=9um

CASE NAME	ENERGY CUTOFF	ESTEP	COMPUTER TIME	DIMENSIONS
C16.IN	1keV with E-library ***el01***	ESTEP= 3	1140min	Radius=10um; Total Thickness=9um
D5.IN	1keV with E-library ***el01***	ESTEP= 3	20min	Radius=10um; Total Thickness=9um
D8.IN	1keV with E-library ***el01***	ESTEP= 3	23hr=1380min	Radius=10um; Total Thickness=9um
D10.IN	1keV with E-library ***el01***	ESTEP=15	66hr=3960min	Radius=10um; Total Thickness=9um
D15.IN	1keV with E-library ***el01***	ESTEP=80	48hr=2880min	Radius=10um; Total Thickness=9um
D16.IN	1keV with E-library ***el03***	ESTEP=80	24hr=1440min	Radius=10um; Total Thickness=9um

Table2: Set of different cases for the PENELOPE and MCNP codes changing the model or some simulation parameters.

Radial dose distributions

Total absorbed dose as a function of radial distance D(r) was calculated using both PENELOPE and MCNP and the results compared with the values obtained with the PITS code by Wilson for the corresponding model.

With PENELOPE a Radial-Dose Function was scored. This Tally is present in the example called PENLAYER and in the created user–codes PENRICO and PEN; it allows calculations of the energy deposited $E_n(r)$ within a small scoring volume as function of radius (r) for each layer or slabs and then divided by the scoring volume (Vol) (Table3) or mass (Vol•density). The radial dose function D(r) is expressed in both D((Gy)/particle) vs. r(radius, μm) and D*((keV/μm^3)/particle) vs. r(radius, μm). The main model is a cylinder with outer radius of 10μm and inside cylinders as described in the

previous section and shown in Figures 1.1 and 1.2. Only in one case, called PENRICO2.INO, did the model present only one cylinder with outer radius of 10μm.

Rout (μm)	0.10	0.30	0.50	0.70	0.90	1.10	1.30	1.50	1.70	1.90
S (μm^2)	0.69	3.02	6.03	9.05	12.06	15.08	18.10	21.11	24.13	27.14
Vol (μm^3)	0.03	0.25	0.50	0.75	1.01	1.26	1.51	1.76	2.01	2.26
Rout (μm)	2.10	2.30	2.50	2.70	2.90	3.10	3.30	3.50	3.70	3.90
S (μm^2)	30.16	33.18	36.19	39.21	42.22	45.24	48.25	51.27	54.29	57.30
Vol (μm^3)	2.51	2.76	3.02	3.27	3.52	3.77	4.02	4.27	4.52	4.78
Rout (μm)	4.10	4.30	4.50	4.70	4.90	5.10	5.30	5.50	5.70	5.90
S (μm^2)	60.32	63.33	66.35	69.37	72.38	75.40	78.41	81.43	84.45	87.46
Vol (μm^3)	5.03	5.28	5.53	5.78	6.03	6.28	6.53	6.79	7.04	7.29
Rout (μm)	6.10	6.30	6.50	6.70	6.90	7.10	7.30	7.50	7.70	7.90
S (μm^2)	90.48	93.49	96.51	99.53	102.54	105.56	108.57	111.59	114.61	117.62
Vol (μm^3)	7.54	7.79	8.04	8.29	8.55	8.80	9.05	9.30	9.55	9.80
Rout (μm)	8.10	8.30	8.50	8.70	8.90	9.10	9.30	9.50	9.70	9.90
S (μm^2)	120.64	123.65	126.67	129.68	132.70	135.72	138.73	141.75	144.76	147.78
Vol (μm^3)	10.05	10.30	10.56	10.81	11.06	11.31	11.56	11.81	12.06	12.32

Table3: Outer Radius R_{out}, Surface S, Volume Vol to be considered to convert D(r) PENELOPE results.

With MCNP the Energy Distribution or *F8 tally, expressed in (MeV/particle), was scored and divided by the volume (cm^3) of each scoring zone (Table 4) in order to match with PENELOPE results. The results are than transformed in both D((Gy)/particle) and D*((keV/μm^3)/particle) unit. In earlier MCNP models the scoring cylinders had height H=1μm and their radius Rout(i) was 1μm off one from the other (defining zones so that $R_{out(i+1)}$- $R_{out(i)}$ = 1μm). Later the number of cylinders has been increased in defining zones so that $R_{out(i+1)}$- $R_{out(i)}$ = 0.2μm keeping H=1μm so that the volumes of each zones of the cell (Table4) are in a better agreement with the number and sizes of scoring volumes of the PENELOPE simulations (Table 3). The increase in the number of scoring volumes in MCNP was made in order to have a possible better comparison with the PENELOPE and PITS results especially for radial distances from 0-5μm were bigger differences were outlined even in earlier cases.

Rout (μm)	0.10	0.30	0.50	0.70	0.90	1.10	1.30	1.50	1.70	1.90		
S (μm^2)	0.69	3.02	6.03	9.05	12.06	15.08	18.10	21.11	24.13	27.14		
Vol (μm^3)	0.03	0.25	0.50	0.75	1.01	1.26	1.51	1.76	2.01	2.26		
Rout (μm)	2.10	2.30	2.50	2.70	2.90	3.10	3.30	3.50	3.70	3.90		
S (μm^2)	30.16	33.18	36.19	39.21	42.22	45.24	48.25	51.27	54.29	57.30		
Vol (μm^3)	2.51	2.76	3.02	3.27	3.52	3.77	4.02	4.27	4.52	4.78		
Rout (μm)	4.10	4.30	4.50	4.70	4.90	5.10	5.30	5.50	5.90			
S (μm^2)	60.32	63.33	66.35	69.37	72.38	75.40	78.41	81.43	100.28			
Vol (μm^3)	5.03	5.28	5.53	5.78	6.03	6.28	6.53	6.79	14.33			
Rout (μm)	6.10	6.50	6.90	7.10	7.50	7.90	8.10	8.50	8.90	9.10	9.50	9.90
S (μm^2)	90.48	110.84	117.87	105.56	128.43	135.47	120.64	146.02	153.06	135.72	163.61	170.65
Vol (μm^3)	7.54	15.83	16.84	8.80	18.35	19.35	10.05	20.86	21.87	11.31	23.37	24.38

Table4: Outer Radius R_{out}, Surface S, Volume Vol to be considered to convert D(r) MCNP results.

The scoring volume for the PITS code is always constant and equal to the volume of a sphere with diameter equal to 2R=1μm.

VolPITS=4/3•π•R^3 =4/3•π•0.5^3 = 0.5236 μm^3

The PITS scoring volume is smaller, if compared to the one adopted for PENELOPE and MCNP, for $\mathbf{R_{out}}$>0.5 μm allowing more detailed information in the region of the cell with Rout from 0.5 to10 μm. For cell radial dimensions from 0 to 0.5μm the PENELOPE and MCNP scoring volume is smaller.

The Radial-Dose Function was scored for all cases in each layer. Figures 3.1-3.9 and 5.1-5.9 present the dose in different units as function of radial distance within each layer from layer1 to layer9. The results data of the 3 codes PENELOPE, MCNP, PITS are compared for the following cases:

+	=PENELOPE 1keV, DSMAX=0.1, C1=0.01, C2=0.01,	(Case PEN02.INO)
O	=MCNP el01, ESTEP=15,	(Case D10.INO)
X	=PITS	(PITS2.DAT from Wilson)

Analysis of Figures 3.1-3.9 and 5.1-5.9 reveals e a good general agreement for the results of the 3 codes for the Radial-Dose Function. Nevertheless, it's important to point out that, in particular for layer 1 and 2, the radial dose in the region from 2 to 4μm presents a considerable difference between the MCNP values against those of PENELOPE and PITS.

The possible reasons for the different profile computed by MCNP against the one computed by PENELOPE and PITS are here presented; efforts have been made to clearly understand and eliminate these differences, if possible.

1. *Monte Carlo method*. As explained in previous sections the two codes deal with electron transport in a different way and this may lead to different results. No attempts were made to modify the structure and nature of the codes.
2. *Energy Cutoff*. Earlier models used the default minimum values for Energy Cutoffs. In particular the PENELOPE energy cutoff for electrons is 100eV, while is 1keV for MCNP. The models that gave the results plotted in Figure 1-9 used instead an electron energy cutoff of 1keV for both codes. No substantial difference in dose profileswas noticed after changing the electron energy cutoff, as presented in the following sections (PENELOPE and MCNP simulations varying some parameters), and still some wide regions of disagreement are present.
3. *ESTEP in MCNP, DSMAX in PENELOPE*. An important parameter for MCNP electron transport is the simulation parameter ESTEP while for PENELOPE the DSMAX parameter might be important to identify the reason of the disagreement. Several models for both codes were created to identify an optimal and suggested use of these parameters for microdosimetric problems. However, the disagreement in data is still big for certain regions of the cell model. More information on these parameters and effects on simulations are presented in the sections called: “PENELOPE and MCNP simulations varying some parameters”.
4. *Size and number of scoring volumes.* In earlier MCNP models the scoring cylinders had a much bigger volume if compared to those of PENELOPE. Although this would not be the actual cause of the disagreement between the codes, smaller volumes, with the consequent increase in number of volumes, were considered for later models allowing an even closer similarity with PENELOPE.
5. *Tally segmentation* is used to subdivide a cell into segments for tallying purpose only. This feature is not applicable for the *f8 tally used in MCNP-4C. The homogeneous phantom had to be subdivided in cells, also called scoring volumes, to calculate the distribution of dose: this was elaborate and may have brought some problems because of small errors introduced during radiation boundary crossing. The repeated interruptions of the electron track at the cell boundaries may happen even in an homogeneous media [9] and this is supposed to significantly

affect the electron transport, although no mention of this is explained in the MCNP –4C manual.

So far the disagreement between the MCNP values against those of PENELOPE and PITS in some regions was not eliminated, but only slightly reduced considering the above points (in particular 2,3,4). It is possible to believe that the modification for tally segmentation that has been carried out in the new version of the code (MCNP-5) from the previous MCNP-4C version could bring better agreement.

The values of D*(r) in keV/μm^3 were computed with the 3 codes PENELOPE, MCNP, PITS and later transformed into D(r) in Gy by means of a constant converting factor (CF=$1.602 \bullet 10^{-1}$).

En=Energy Imparted, m/Vol/d=mass/volume/density of the scoring volume

D=En/m m=Vol•d

D*=En/Vol

=>D=D*/d

Since D is expresses in Gy =J/kg while D* in keV/μm^3 the following must apply:

D(Gy)=D*(keV/μm^3)•$1.602 \bullet 10^{-1}$ (Gy•μm^3/keV)

Depth dose distributions

Total absorbed dose as function of penetration ***D(x)*** was calculated using both PENELOPE and MCNP and the results compared with the values obtained with the PITS code by Wilson for the corresponding model. The Depth-Dose Function was scored for all cases but not plotted separately since it is included on the 3-D plot of the dose distributions of Figures 4.1, 4.2, 4.3 and Figures 6.1, 6.2, 6.3. In these cases the energy deposited is divided by the mass or by the volume.

With PENELOPE the depth-dose function ***D(x)*** is expressed in D((keV/μm)/particle) vs. x(depth, μm). The main model has 9 layers, each layer being 1μm thick for a total thickness of 9μm. 50 Dose Data Points are plotted for the respected values of depth within each slab for a total of 450 data

points every 0.02μm within the entire cell. These values are valid for the simulation cases called PENRICO4.INO, from PENRICO8.INO to PENRICO11.INO, PEN01.INO, PEN02.INO, PEN03.INO (cases plotted). Only for three cases (called PENRICO1.INO, PENRICO2.INO, PENRICO3.INO) one layer of 10μm total thickness is considered. This allows having 50 Dose Data Points plotted for the respected values of depth every 0.2μm. For the simulation cases from PENRICO5.INO to PENRICO7.INO, 9 layers for a total thickness of 4.5μm are considered; each layer being 0.1μm thick.

With MCNP the Energy Distribution or *F8 tally, expressed in (MeV/particle), was scored and divided by the total thickness of the layer (cm) of each zone in order to match with PENELOPE results. The results are than transformed into the D(keV/μm)/particle) vs. x(depth, μm) unit.

3-D plot of the dose distributions

Figures 4.1, 4.2, 4.3 and Figures 6.1, 6.2, 6.3 present the absorbed dose ***D(r,x)*** as function of radial distance ***r*** and of penetration ***x*** summarizing, respectively, the PENELOPE, MCNP, PITS results for the 9 layers of Figures 3.1-3.9 and Figures 5.1-5.9.

PENELOPE simulations varying some parameters

The PENELOPE code has been used varying some of the simulations parameters: Energy Cutoff, C1, C2, WCC, WCR, DSMAX.

The ***Energy Cutoff*** for this problem has been changed in the INPUT file in two different set of cases using 100 eV or 1 keV for electrons. The 1 keV value has been selected to see the effect of the energy cutoff compared to the 100 eV value and to find a better comparison with the MCNP code that has an electron Energy Cutoff of 1keV.

The ***input parameter C1*** is the average angular deflection produced by multiple elastic scattering along a path length equal to the mean free path between hard elastic events. The maximum maximum allowed value is 0.2, with a minimum value of 0 , and normally a value of the order of 0.01 is adequate.

The ***input parameter C2*** is the maximum average fractional energy loss between consecutive hard elastic events. The maximum C2 value allowed is 0.1, with a minimum value of 0 , and normally a value of the order of 0.01 is adequate.

The ***input parameter WCC*** is the cutoff energy loss (in eV) for hard inelastic collisions while ***WCR*** is the cutoff energy loss (in eV) for hard Bremsstrahlung emission.
The values of WCC and WCR are both set to be 100eV in all simulations performed.

These parameters determine the accuracy and speed of the simulation. To ensure accuracy, C1 and C2 should have small values (of the order of 0.01 or so). With larger values of C1 and C2 the simulation gets faster, at the expense of a certain loss in accuracy. The cutoff energies WCC and WCR mainly influence the simulated energy distributions. The simulation speeds up by using larger cutoff energies, but if these are too large, the simulated energy distributions may be somewhat distorted. **[c1, p7]**

To change the ***value of DSMAX*** it is necessary to modify the user-code that needs to be compiled and linked to PENELOPE.for file: the user-code PENRICO.for has a DSMAX=10^{35} while PEN.for has a DSMAX=0.1.

The input parameter DSMAX defines the maximum allowed step length for electrons/positrons; for photons, it has no effect. To limit the step length, PENELOPE places delta interactions along the particle track. These are fictitious interactions that do not alter the physical state of the particle. Their only effect is to interrupt the sequence of simulation operations (which requires altering the values of inner control variables to permit resuming the simulation in a consistent way). The combined effect of

the soft interactions that occur along the step preceding the delta interaction is simulated by the usual random-hinge method. Owing to the Markovian nature of hard interactions, the introduction of delta interactions does not alter the distribution of path lengths between consecutive hard events. To ensure the reliability of the mixed simulation algorithm, the number of artificial soft events per particle track in each body should be larger than 10. For relatively thick bodies (say, thicker than 10 times the mean free path between hard interactions), this condition is automatically satisfied. In this case we can switch off the step length control by setting DSMAX=1.0^{35} (large value). On the other hand, when the particle moves in a thin body, DSMAX should be given a value of the order of one tenth of the thickness of that body. **[c1, p8….]**

Energy Cutoff=100eV, 1keV
WCC=100eV
WCR=100eV
C1=0, 0.01, 0.05
C2=0.01, 0.05
DSMAX = off (MAX), 0.1

Figures 7.1-7.4 present the PENELOPE results for dose deposited as function of radial distance within some layers and zooming in a particular radial zone to show the effect of the different parameters on the final output. The simulation parameters of the PENELOPE code are changed and the results data are compared for the following cases:

+ =PENELOPE 100eV,DSMAX max, C1=0.05, C2=0.05, 75600 SEC [case penrico9.ino]
- =PENELOPE 1KeV, DSMAX max, C1=0.05, C2=0.05, 3600 SEC [case penrico10.ino]
-- =PENELOPE 1keV, DSMAX=0.1, C1=0.01, C2=0.01, 1800 SEC [case pen02.ino]
-. =PENELOPE 100eV,DSMAX=0.1, C1=0.00, C2=0.01, 3600 SEC [case pen03.ino]
0 =PITS

It is very difficult to underline the differences between the cases on the plots of Figures 7.1-7.4 and it seems that the effect of the parameters is often negligible when computing only the radial Dose distribution inside the cylindrical scoring volume used for this problem. In fact it is not enough to use a single dose number for each particular radial zone, and other quantities needs to be tallied as explained in the conclusions

MCNP simulations varying some parameters

The MCNP code has been used varying the ESTEP parameter and trying different electron library.
The ***electron library*** contains data on an element-by-element basis for atomic numbers Z=1-94 and there is no distinction between isotopes for a given element. The library data contain energies for tabulation, radioactive stopping power parameters, Bremsstrahlung production cross sections, Bremsstrahlung energy distributions, K-edge energies, Auger electron production energies, parameters for the evaluation of the Goudsmit-Saunderson theory for angular deflections based on the Riley cross section calculation, and Mott correction factors to the Rutherford cross sections also used in the Goudsmit-Saunderson theory.

The el03 database also includes the atomic data of Carlson used in the density effect calculation. Internally, calculated data are electron stopping powers and ranges, K x-ray production probabilities, knock-on probabilities, Bremsstrahlung angular distributions, and the Landau-Blunck-Leisegang theory of energy-loss fluctuations. The el03 evaluation is derived from the ITS3.0 code system.[c10, c11]

ESTEP causes the number of electron sub-steps per energy step to be increased for the material. The condensed random walk for electrons is structured in terms of *major steps* or *energy step*s. The representation of the electron's trajectory as the result of many small steps will be more accurate if the angular deflections are also required to be small. Therefore, the MCNP codes further break the electron steps into smaller sub-steps. A major step of path length s is divided into m substeps, each of path length $s/$m. Angular deflections and the production of secondary particles are sampled at the level of these sub-steps. The integer m depends only on material (average atomic number Z). Appropriate values for m have been determined empirically, and range from $m = 2$ for $Z < 6$ to $m = 15$ for $Z > 9$1. In some circumstances, like for our case, it may be desirable to increase the value of m for a given material. In particular, a very small material region may not accommodate enough sub-steps for an accurate simulation of the electron's trajectory. In such cases, the user can increase the value of m with the ESTEP option on the material card. A reasonable rule of thumb is that an electron should make at least ten sub-steps in any material of importance to the transport problem. [c2 p2-65].

Figures 8.1-8.4 present the MCNP results for dose deposited as function of radial distance within some layers and zooming in a particular radial zone to show the effect of the different parameters on the final

output. The simulation parameters of the MCNP code are changed and the results dta are compared for the following cases:+ =MCNP el01, ESTEP= 3, 23hr=1380min [case D8.INO]

- =MCNP el01, ESTEP=15, 66hr=3960min [case D10.INO]

-- =MCNP el01, ESTEP=80, 48hr=2880min [case D15.INO]

-. =MCNP el03, ESTEP=80, 24hr=1440min [**case** D16.INO]

0 =PITS

As explained in the previous paragraph, it is very difficult to underline the differences between the cases on the plots of Figures 8.1-8.4 because other quantities need to be tallied and analyzed.

3-D plot of the track simulation using MCNP

Figures 2.1, 2.2, 2.3 present the simulation of Electrons tracks within the cylindrical cell considering all the collision points given by the MCNP code. In particular the figures refer to 4 tracks (Figure 2.1), all simulated tracks in the cell (Figure 2.2), and all simulated tracks in the cell and what scatters out (Figure 2.3) for the case called D10.INO (MCNP el01, ESTEP=15, 66hr=3960min).

One can expect that for a large number of histories (and of tracks), tracks are equally distributed along same cylindrical radius (for a selected Z value). This can be identified from the cylindrical symmetry in track distributions of Figures 2.2, 2.3.

CONCLUSIONS

These calculations show the different performances of PENELOPE, MCNP 4C and PITS codes for the evaluation of Dose profiles.

First of all it must be noticed that, although the overall cylindrical cell model is equivalent for the three codes, the internal scoring geometry is different: (water filled cylindrical shells for PENELOPE and MCNP, while spheres for PITS); this doesn't allow an exact and fair comparison between the codes.

As mentioned in PART II the evaluated dose is still a macroscopic quantity and the profiles of the radial dose distribution show data points that are single dose values for each particular radial zone. These values are only integrals and therefore not enough information will assure that at the microscopic level the values are still comparable. In particular the energy spectra might have different shapes and peaks, even if the corresponding area underneath is equivalent or very close.

Nevertheless this preliminary work has been important because it demonstrate that codes like PENELOPE can be used for dose evaluation even with such small sizes and energies involved which are far below the normal use for which the code was created.

Microdosimetry is a field where track-structure codes are believed to be superior. If general-purpose Monte Carlo codes with a mixed algorithm like PENELOPE can prove to provide valid answers, using them can draw several advantages as explained in more details in PART I and here summarized:

1) easier and generally free availability;
2) normally it's more user-friendly, especially if compared with a code created ad hoc for a specific problem;
3) possibility to have answers for many materials other than water
4) more widespread (suggestions and "bug discovery")
5) more frequent up-grades and benchmark from the authors and from the users and thanks to the interaction of both.

For this application PENELOPE appeared to be faster than PITS and MCNP thanks to the mixed simulation algorithm and to the combination of numerical total cross sections (or stopping cross

sections) with simple analytical formulas to get, in a much faster way, the cross sections data. Also PITS simulations took hundreds of hours of computer time while meaningful results were obtained with PENELOPE in less than an hour calculations, and with MCNP a few hours' calculation time.

In conclusion from the simulations performed it turns out that PENELOPE, in particular, has an overall very good response, and it compares well with PITS if only the overall dose values are considered for this application.

FUTURE DIRECTIONS

The study presented here has stimulated our interest in pursuing the work further. Several collaborators have also expressed interest in working with us. Listed below are an indication of some of the future tasks we have outlined for completion:

1. To benchmark PENELOPE general-purpose Monte Carlo code with the track Monte Carlo code PITS in collaboration with Walt Wilson.
2. To create a PENELOPE user-code that could model individual cells with spherical scoring volumes inside.
3. To score microdosimetric quantities within these spheres. In particular Frequency-Mean Specific Energy (Gy) and Event Frequency spectra in Specific Energy (Gy) would be of interest.
4. To obtain radial profiles for Frequency-Mean Specific Energy (Gy) and Dose (Gy).
5. To Compare PENELOPE results with those obtained with PITS and reported in [2].
6. To consider parallel computing in case the statistics of the simulation for the entire geometry isn't accurate enough.
7. To consider comparisons of dosimetric estimates with other track codes such as OREC, ESLOW.
8. To adopt the same codes and models to simulate a 12.5 keV photon microbeam.
9. To benchmark the computations for the 12.5 keV photon against experiments performed at that energy at LBNL's ALS .
10. To improve the geometrical model of a real single cell and simulate a cluster of cells.

ACKNOWLEDGEMENTS

Although this report will be printed in September 2002 it includes mainly some of the results from the simulation work performed at LBNL during Summer 2001 that has been valuable as a learning process for subsequent studies.

Enrico Mainardi wishes to thank the Environmental, Health and Safety Division (EH&S) for the kind hospitality, encouragement and funds that sponsored his visit at LBNL. He is particularly grateful to Dr. Gary Zeman the Radiological Control Manager. Particular thanks to Richard Donahue and Eleanor Blakely who have been very supportive and helpful advisors in this project. This work was also made possible by a fellowship of the Italian Government to attend the Ph.D. program in Energetic at the University of Rome "La Sapienza" without which it would have not been possible to be invited at LBNL. Thank also to Professor Maurizio Cumo to allow this Summer visit to USA and for the opportunity to work, in the field of Monte Carlo radiation transport and modeling both in Rome and at LBNL. Thanks also to Dr. Alessandro Campa of the Istituto Superiore di Sanita' in Rome for the discussions and suggestions.

The authors acknowledge the important contribution of Prof. Francesc Salvat and his team in Barcelona for promptly sending us the PENELOPE main code and for the comments and suggestions. Also essential were the suggestions, data and help from Dr. Wilson of Washington State University at Richland (WSU) who is the author of the PITS code and one of the most knowledgeable and important contributors in the field of microdosimetry. The discussions with Dr. Aloke Chatterjee and Dr. William Holley have been also very valuable throughout the work and especially at the beginning when we were looking for available Monte Carlo codes to simulate photons and electron transport in the micron scale and for lower energies.

REFERENCES

[1] ICRU (1983) Report 36. Microdosimetry. International Commission on Radiation Units and Measurements, Bethesda MD 20814

[2] W. E. Wilson, D.J. Lynch, K. Wei, L.A. Braby. Microdosimetry of a 25keV Electron Microbeam, Radiat. Res. (2001) 155: pp 89-94.

[3] J. H. Miller, M. Sowa Resat, N.F. Metting, K. Wei, D.J. Lynch, W.E. Wilson. Monte Carlo simulation of single-cell irradiation by an electron microbeam, Radiat. Environ. Biophysics (2000) 39: pp 173-177.

[4] W. E. Wilson and H. Nikjoo. A Monte Carlo code for positive ion track simulation. Radiat Environ Biophys 38: 97-104, Radiat. Environ. Biophysics, (1999) 38: pp 97-104.

[5] H. Nikjoo, M. Terrissol, R.N. Hamm, J.E. Turner, S. Uehara, H.G. Paretzke, D.T. Goodhead. Comparison of energy deposition in small cylindrical volumes by electrons generated by Monte Carlo track structure codes for gaseous and liquid water. Radiation Protection Dosimetry, (1994) 52(1-4): pp 165-169.

[6] J.E. Turner, J.L. Magee, H.A. Wright, A. Chatterjee, R.N. Hamm, R.H. Ritchie, Physical and chemical development of electron tracks in liquid water. Radiat. Res., (1983) 96: pp 437-449.

[7] D.T. Goodhead. Relationship of microdosimetric techniques to applications in biological systems. The Dosimetry of Ionizing Radiation, volume 2, chapter 1, pp 1-89. Academic Press, San Diego, (1987).

[8] M. Zaider and H.H. Rossi. Microdosimetry and its applications to biological processes. The Dosimetry of Ionizing Radiation, volume 2, chapter 4, pp 171-242. Academic Press, San Diego, (1987).

[9] Schaart D.R., Jansen J.T., Zoetelief J., Leege P. A comparison of MCNP4C electron transport with ITS 3.0 and experiment at energies between 100 keV and 20 MeV: Influence of voxel size, substeps and energy indexing algorithm. Submitted for publication in Phys. Med. Biol. 2002.

[10] Stewart, RD, Wilson, WE, McDonald, JC, and Strom, DJ, Microdosimetric properties of ionizing electrons in water: a test of the PENELOPE code system. Phys. Med. Biol. 2002, Jan 7:47(1);79-88.

[11] Mothersill, C. and Seymour C. B., Radiation-induced bystander effects: Past history and future directions, Radiat. Res. 155,759-767, 2001.

[12] Mothersill, C., Seymour, C. B. and Joiner, M.C. Relationship between radiation-induced low-dose hypersensitivity and the bystander effect, Radiat. Res. 157, 526-532, 2002

[13] Attix F.H., Introduction to radiological physics and radiation dosimetry. Wiley-Interscience.

CODE REFERENCES

[c1] F. Salvat, J.M. Fernandez-Varea and J. Sempau, 'PENELOPE, an algorithm and computer code for Monte Carlo simulation of electron-photon showers', Version 2000.08.28.

[c2] J. F. Briesmeister editor, 'MCNP - A General Monte Carlo N-Particle Transport Code', Version 4C, La-13709-m Manual, March 2001, Los Alamos National Laboratory.

[c3] W.E. Wilson, J.H. Miller and H. Nikjoo, "PITS: A Code Set for Positive Ion Track Structure", In Computational Approaches in Molecular Radiation Biology, (Ed. M.N. Varma and A. Chatterjee) Plenum Press, New York, (1994), pp 137-153.

[c4] W.E. Wilson and H. Nikjoo, "A Monte Carlo code for positive ion track simulation", Radiat. Environ. Biophys, (1999) 38: pp 97-104.

[c5] TART: D.E. Cullen, 'TART97: A Coupled Neutron-Photon 3-D, Combinatorial Geometry Monte Carlo Transport Code,' Lawrence Livermore National Laboratory, UCRL-ID-126455, Rev. 1, November, 1997.

[c6] EGS4: Nelson W.R., Hirayama H., Rogers D.W.O. (1985). The EGS4 code system (SLAC report 265)

[c7] EGS4: Nelson W.R.and Rogers D.W.O. (1985). Structure and operation of the EGS4 code system. In T.M. Jenkins et al., editors, Monte Carlo Transport of Electrons and Photons, chapter 12. Plenum Press, New York.

[c8] ETRAN: Berger MJ, Seltzer SM (1973) Etran, Monte Carlo code system for electron and photon transport through extended media ORNL. Documentation for RISC computer code package CCC-107

[c9] ETRAN: Stephen M. Seltzer, "An Overview of ETRAN Monte Carlo Methods," in Monte Carlo Transport of Electrons and Photons, edited by Theodore M. Jenkins, Walter R. Nelson, and Alessandro Rindi, (Plenum Press, New York, 1988) 153.

[c10] ITS: J. Halbleib, "Structure and Operation of the ITS Code System," in Monte Carlo Transport of Electrons and Photons, edited by Theodore M. Jenkins, Walter R. Nelson, and Alessandro Rindi, (Plenum Press, New York, 1988) 249.

[c11] ITS Code Manual. F. Him. Radiation Information and Shielding Center, 1992.

[c12] ITS-TIGER: J. A. Halbleib, R. P. Kensek, T. A. Mehlhorn, G. D. Valdez, S. M. Seltzer, and M. J. Berger, "ITS Version 3.0: The Integrated TIGER Series of Coupled Electron/Photon Monte Carlo Transport Codes", Sandia National Laboratories report SAND91-1634 (March 1992).

[c13] PTRAN: Berger MJ (1993) Proton Monte Carlo transport programme PTRAN. (Report NISTIR-5113) National Institute of Standards and Technology, Gaithersbury, MD
[c14] MOCA8b: Paretzke HG (1987) Radiation track structure theory. In: Freeman GR (ed) Kinetics of nonhomogeneous processes. John Wiley, New York, pp 89–170
[c14b] MOCA8b: Paretzke H.G.. Simulation von elektronenspuren im energiebereich 0.01-10 keV. In Wasserdampf Gesellschaft f. ur Strahlen-und Umwelt Forschung M. unchen, pages 24-88. GSF-Bericht, 1988.
[c15] MOCA14: Wilson WE, Paretzke HG (1981) Calculation of distribution of energy imparted and ionizations by fast protons in nanometer sites. Radiat Res 81: 521–537
[c16] OREC: Hamm RN, Turner JE, Ritchie RH, Wright HA (1985) Calculation of heavy-ion tracks in liquid water. Radiat Res 104: S20–S26
[c17] OREC: R.N. Hamm, H.A. Wright, J.E. Turner, and R.H. Ritchie. Spatial correlation of energy deposition events in irradiated liquid water. In Proceedings of the Sixth Symposium on Micro-dosimetry, pages 178-186, Brussels, 1978. Commission of the European Communities.
[c18] CPA100: Terrissol M, Beaudre A (1990) Simulation of space and time evolution of radiolytic species induced by electrons in water. Radiat Prot Dosim 31: 171–175
[c19] CPA100: M. Terrisol, J.P. Patau, and T. Eudaldo. Application a la microdosimetrie et a la radiobiologie de la simulation du transport des electrons de basse energie dans l'eau liquide. In Proceedings of the Sixth Symposium on Microdosimetry, pages 169-178, Brussels, 1978. Commission of the European Communities.
[c20] DELTA: Zaider M, Brenner DJ, Wilson WE (1983) The applications of track calculations to radiobiology. 1. Monte Carlo simulation of proton tracks. Radiat Res 95: 231–247
[c21] ETRACK: Ito A. (1987) Calculation of double-strand break probability of DNA for low LET radiations based on track structure analysis. Nuclear and atomic data for radiotherapy and related radiobiology STI/PUB/741. International Atomic Energy Agency, Vienna, pp 413–429
[c22] ETRACK: Ito A. (1988) Electron track simulation for microdosimetry. In T.M. Jenkins et al., editors, Monte Carlo Transport of Electrons and Photons, chapter 16. Plenum Press, New York.
[c23] KURBUC: Uehara S, Nikjoo H, Goodhead DT (1993) Cross-sections for water vapour for Monte Carlo track structure code from 10 eV to 10 MeV region. Phys Med Biol 38: 1841–1858
[c24] TRION: Lappa AW, Bigildev EA, Burminstrov DS, Vasilyev ON (1993) Trion code for radiation action calculations and its ap-plication in microdosimetry and radiobiology. Radiat Environ Biophys 32: 1–19

[c25] ESLOW: T.M. Evans (October 1997), The Measurement and Calculation of Nanodosimetric Energy Distributions for Electrons and Photons, Ph.D. Thesis (Georgia Institute of Technology Neely Nuclear Research Center Atlanta, GA)

List of Figures

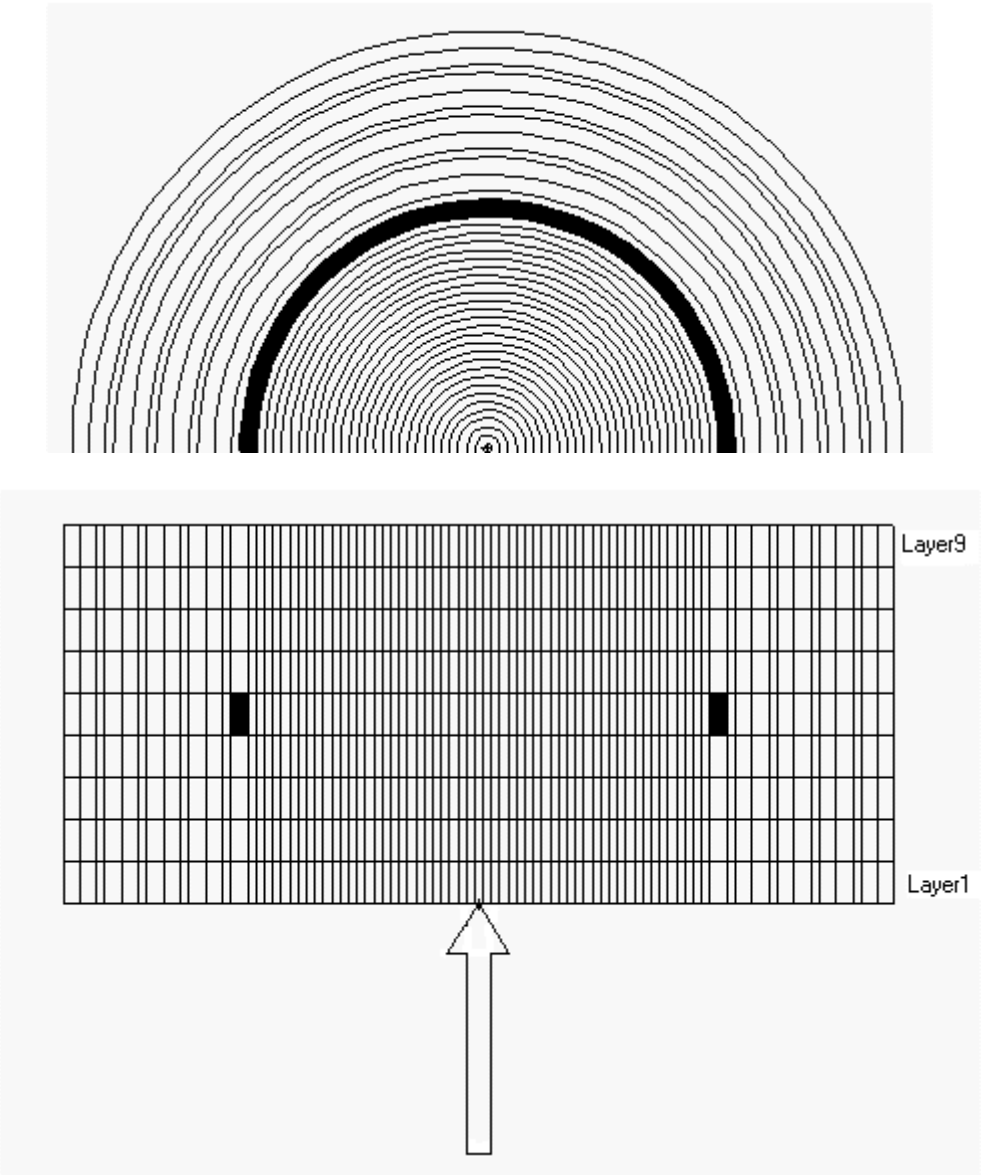

Figures 1.1, 1.2: Geometrical model of a biological cell. Radial and Vertical view of the cylindrical model of a cell used for MCNP and PENELOPE calculations. The zones of the cell are also refered as scoring volumes with the shape of hollow cylinders for each Layer. In black the scoring volume for Layer5 (4-5μm) and Radial Distance 5.5-5.9μm.

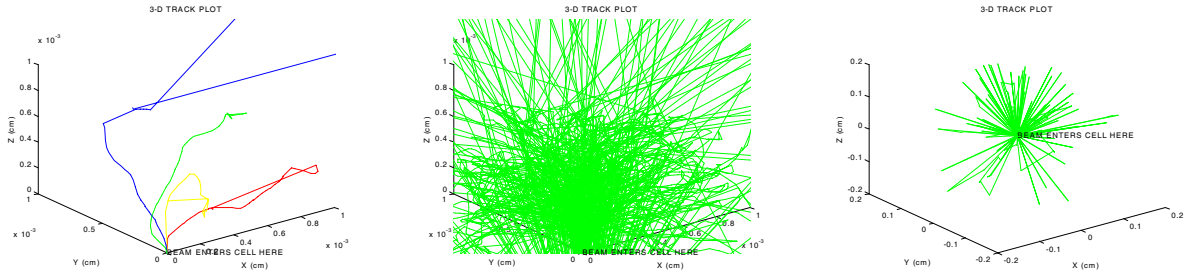

Figures 2.1, 2.2, 2.3: 3-D plot of the track simulation (from MCNP output)

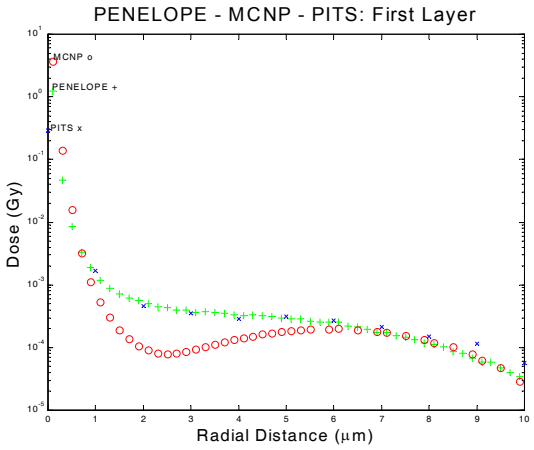
PENELOPE - MCNP - PITS: First Layer
MCNP o
PENELOPE +
PITS x
Dose (Gy)
Radial Distance (μm)

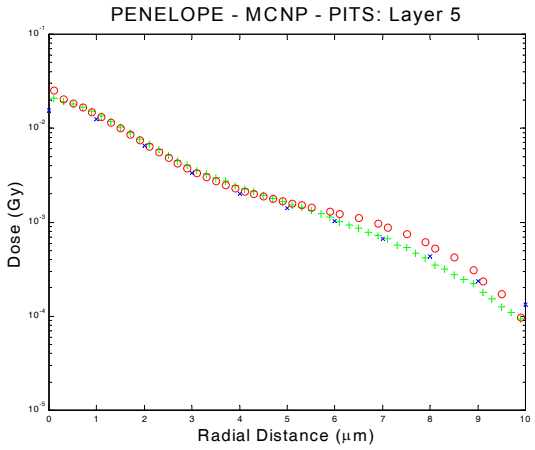
PENELOPE - MCNP - PITS: Layer 5
Dose (Gy)
Radial Distance (μm)

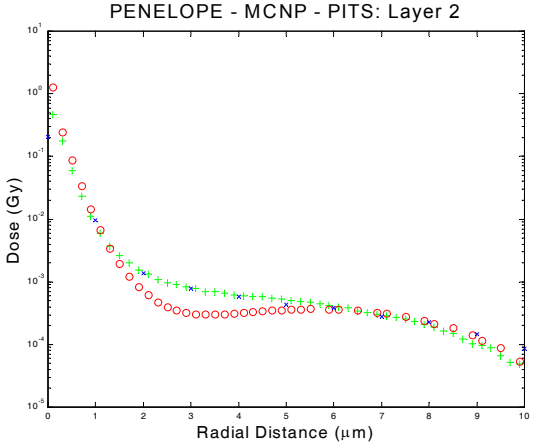
PENELOPE - MCNP - PITS: Layer 2
Dose (Gy)
Radial Distance (μm)

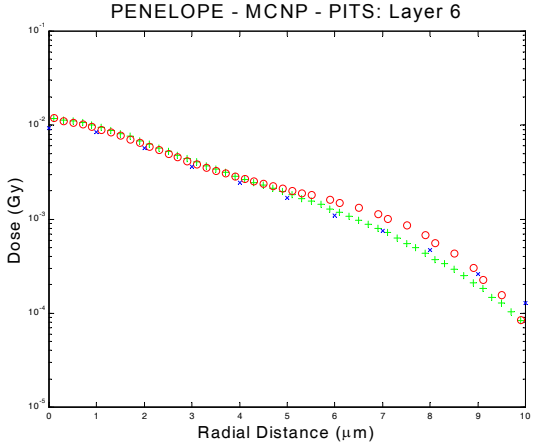
PENELOPE - MCNP - PITS: Layer 6
Dose (Gy)
Radial Distance (μm)

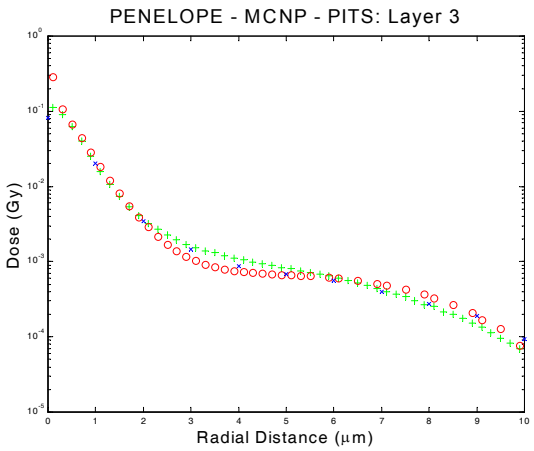
PENELOPE - MCNP - PITS: Layer 3
Dose (Gy)
Radial Distance (μm)

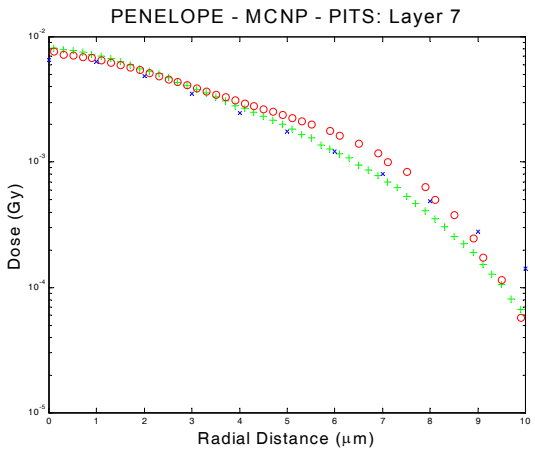
PENELOPE - MCNP - PITS: Layer 7
Dose (Gy)
Radial Distance (μm)

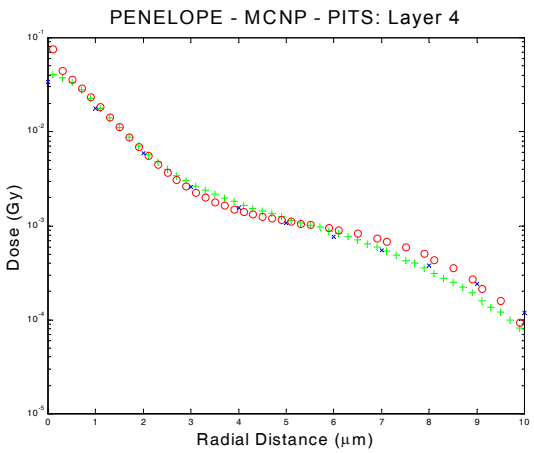
PENELOPE - MCNP - PITS: Layer 4
Dose (Gy)
Radial Distance (μm)

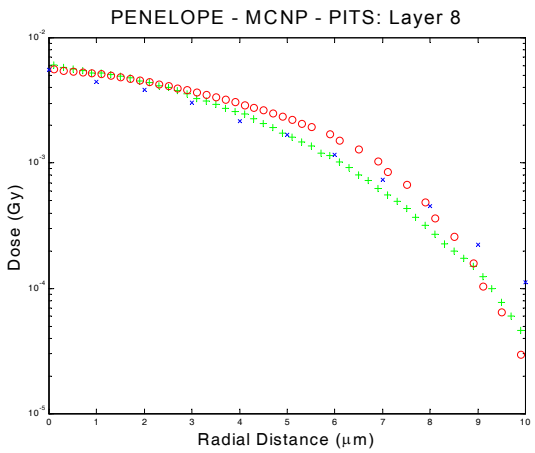
PENELOPE - MCNP - PITS: Layer 8
Dose (Gy)
Radial Distance (μm)

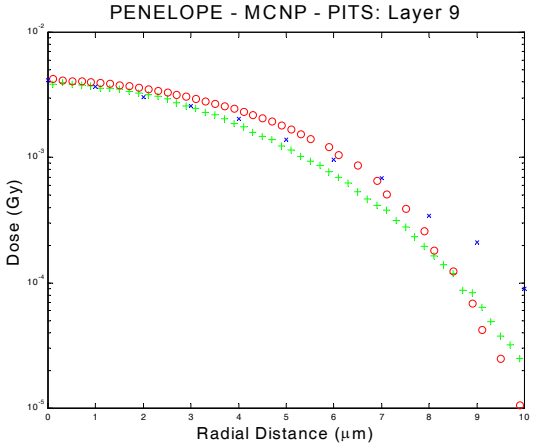

Figures 3.1 – 3.9: PENELOPE, MCNP, PITS 2-D plots of radial dose distributions **D(r)** in **(Gy)**. Each figure represent a comparison of D(r) values computed with the three codes and for each layer 1μm thick.

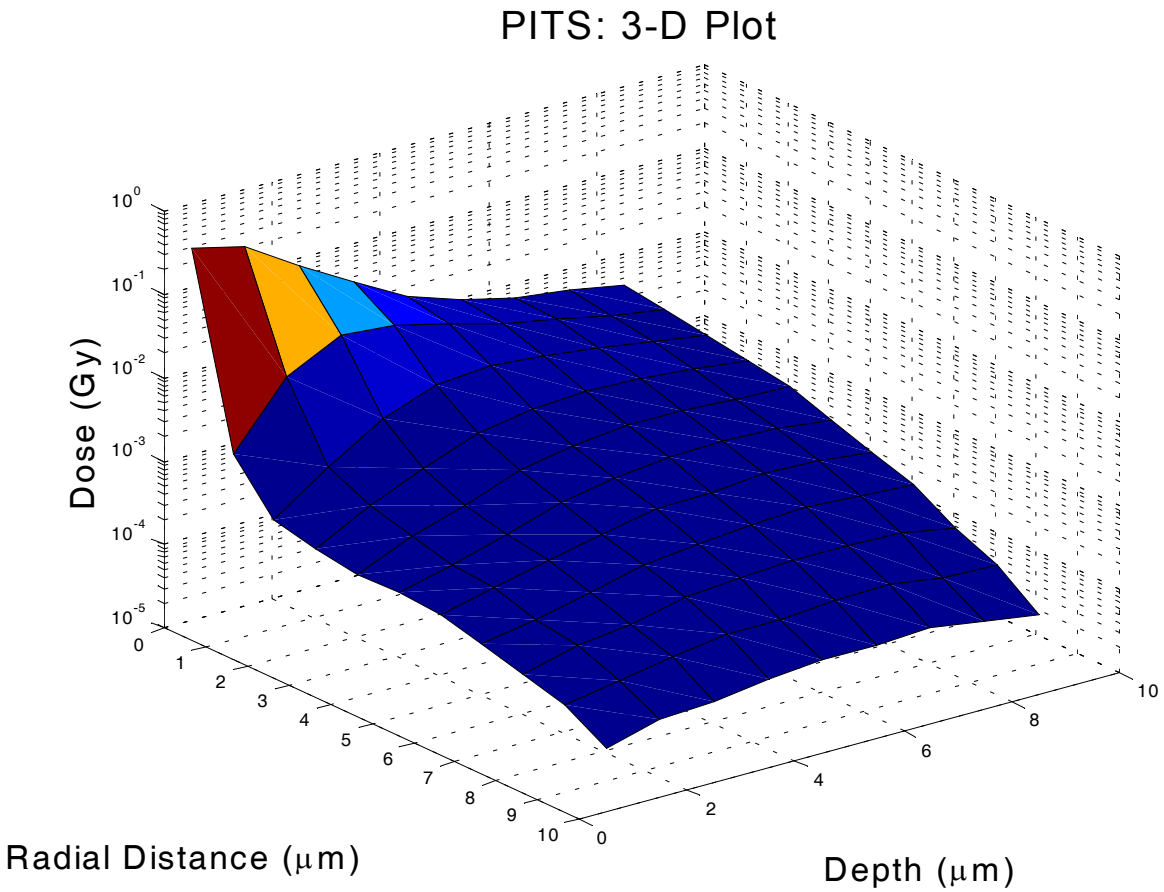

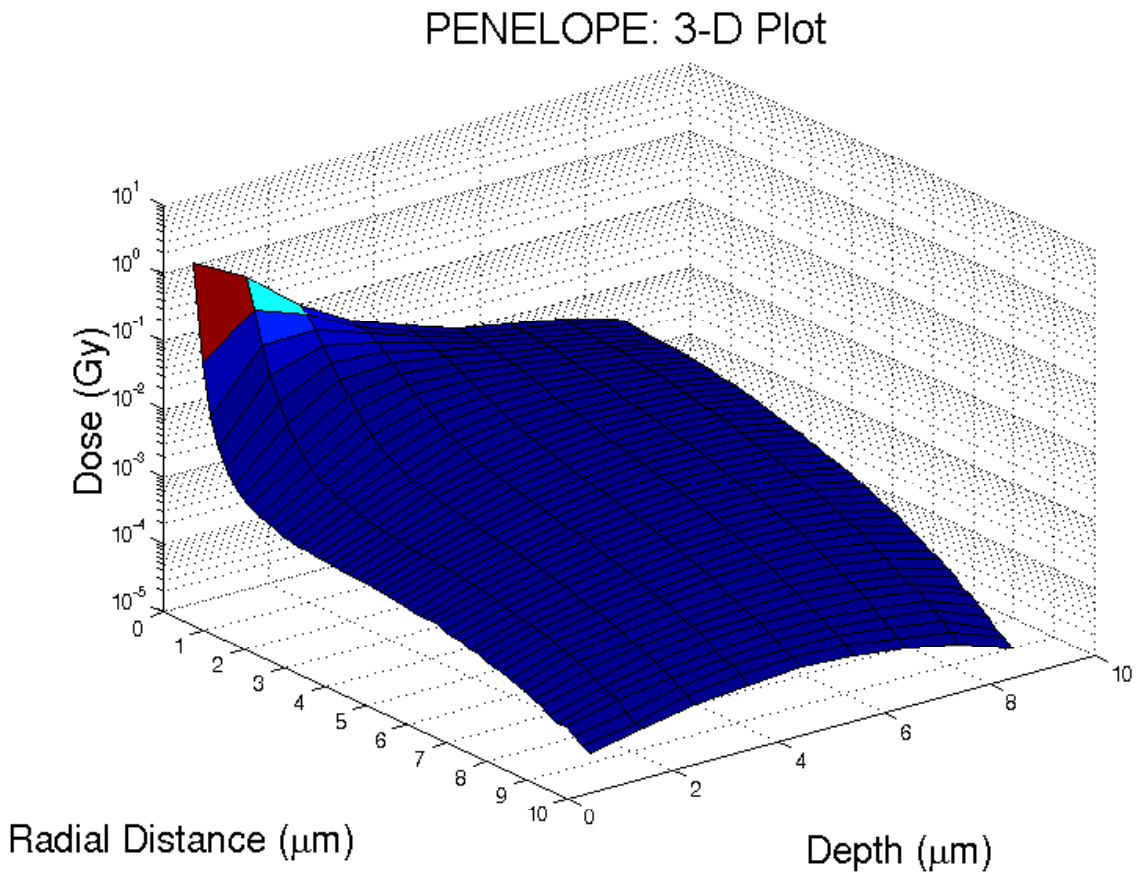

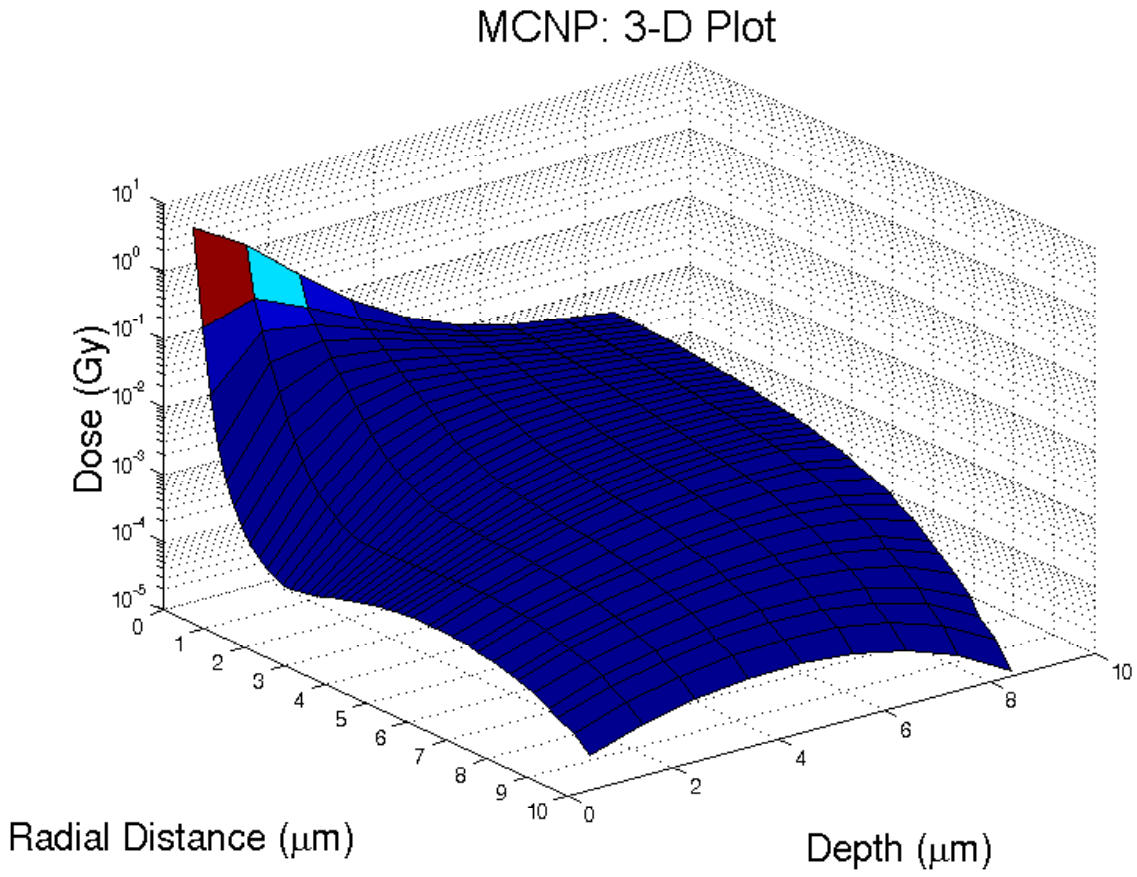

Figures 4.1 – 4.3: 3-D plots of dose distributions **D(r,x)** in **(Gy)** as function of radial distance (r) and of penetration (x) for each code: PENELOPE, MCNP, PITS.

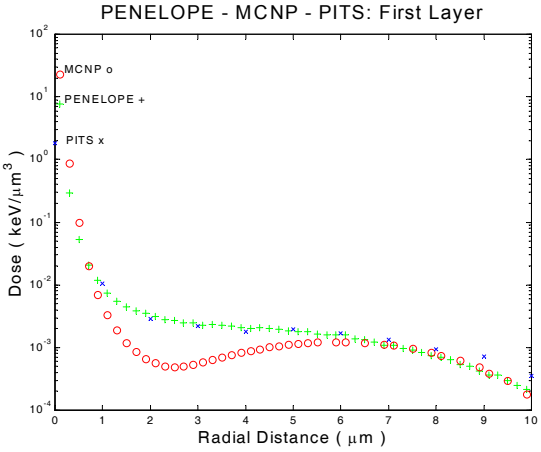
PENELOPE - MCNP - PITS: First Layer
MCNP o
PENELOPE +
PITS x
Dose (keV/μm3)
Radial Distance (μm)

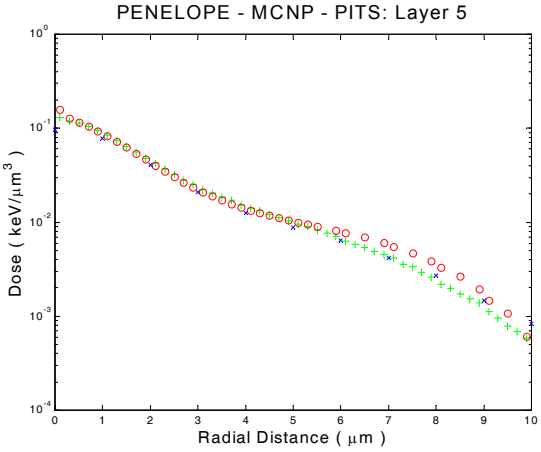
PENELOPE - MCNP - PITS: Layer 5
Dose (keV/μm3)
Radial Distance (μm)

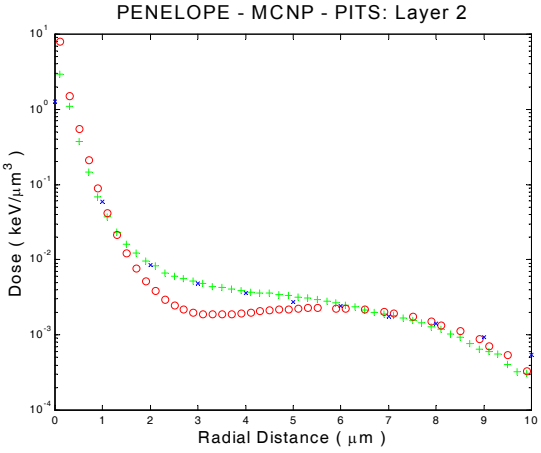
PENELOPE - MCNP - PITS: Layer 2
Dose (keV/μm3)
Radial Distance (μm)

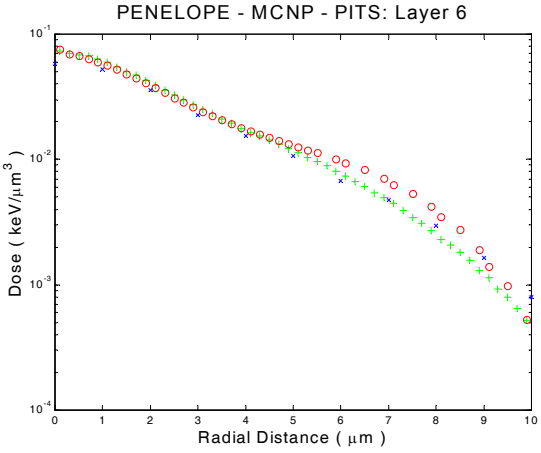
PENELOPE - MCNP - PITS: Layer 6
Dose (keV/μm3)
Radial Distance (μm)

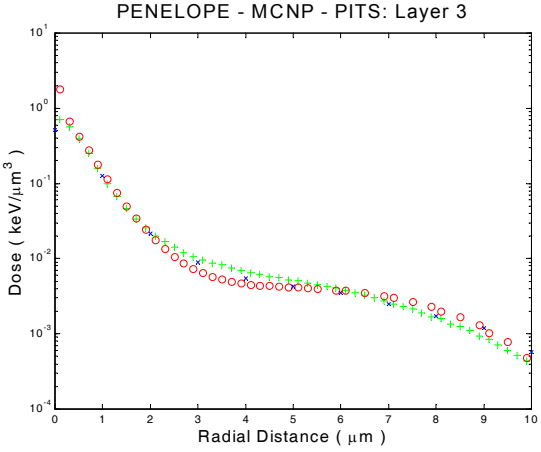
PENELOPE - MCNP - PITS: Layer 3
Dose (keV/μm3)
Radial Distance (μm)

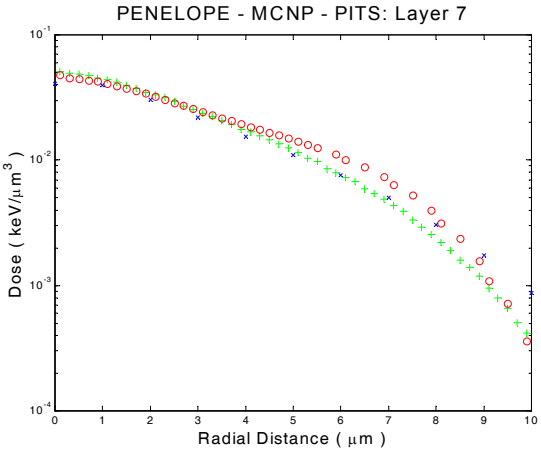
PENELOPE - MCNP - PITS: Layer 7
Dose (keV/μm3)
Radial Distance (μm)

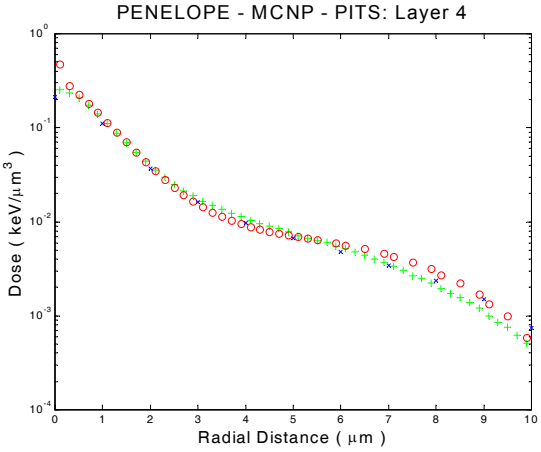
PENELOPE - MCNP - PITS: Layer 4
Dose (keV/μm3)
Radial Distance (μm)

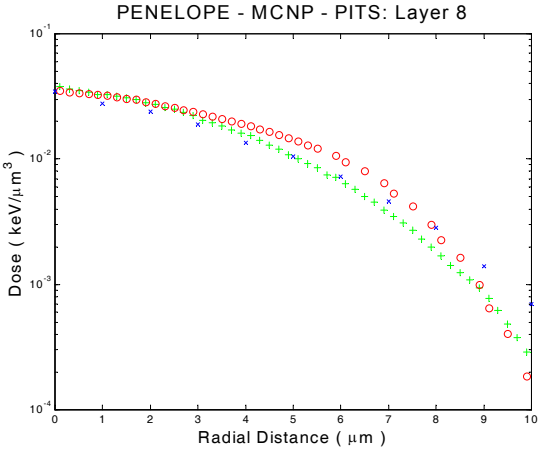
PENELOPE - MCNP - PITS: Layer 8
Dose (keV/μm3)
Radial Distance (μm)

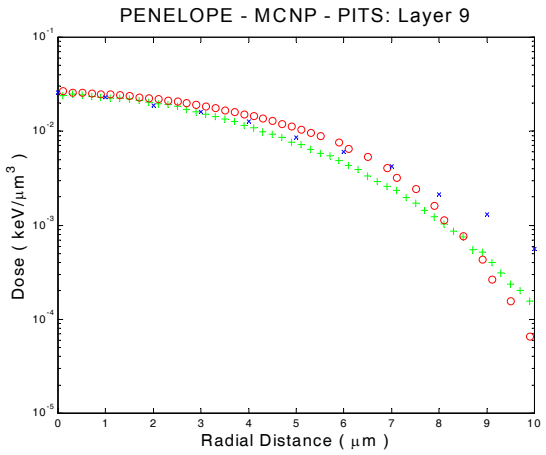

Figures 5.1 – 5.9: PENELOPE, MCNP, PITS 2-D plots of radial dose distributions **D(r)** in **(keV/μm^3)**. Each figure represent a comparison of D(r) values computed with the three codes and for each layer 1μm thick.

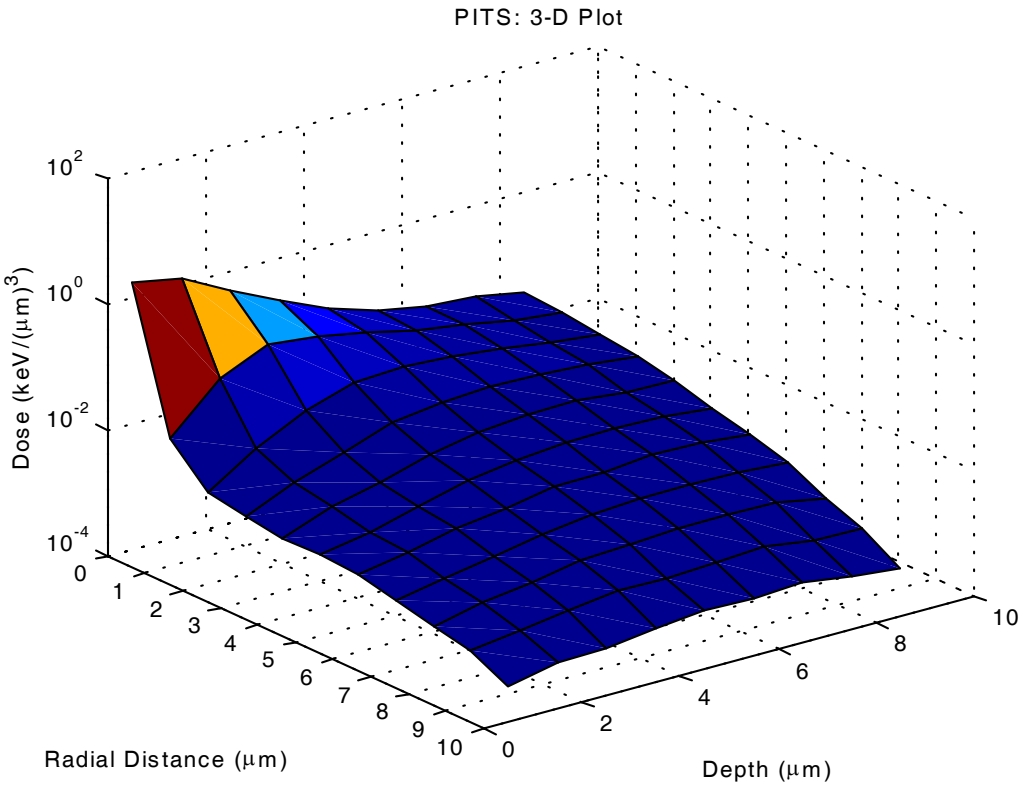

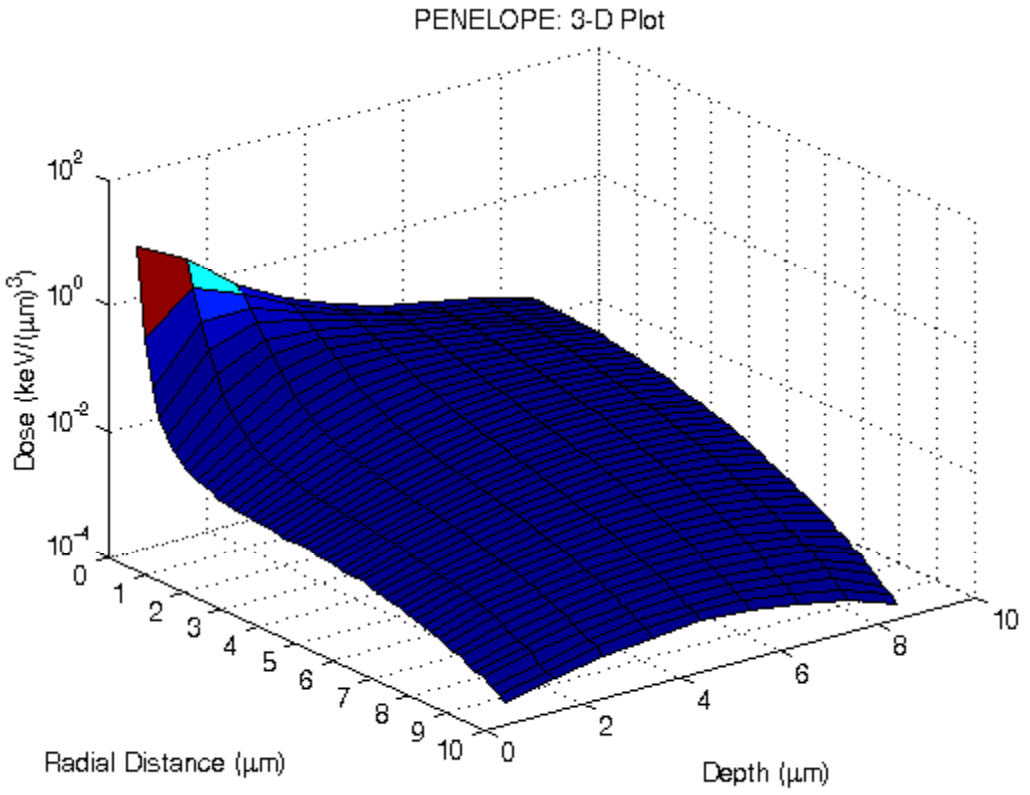

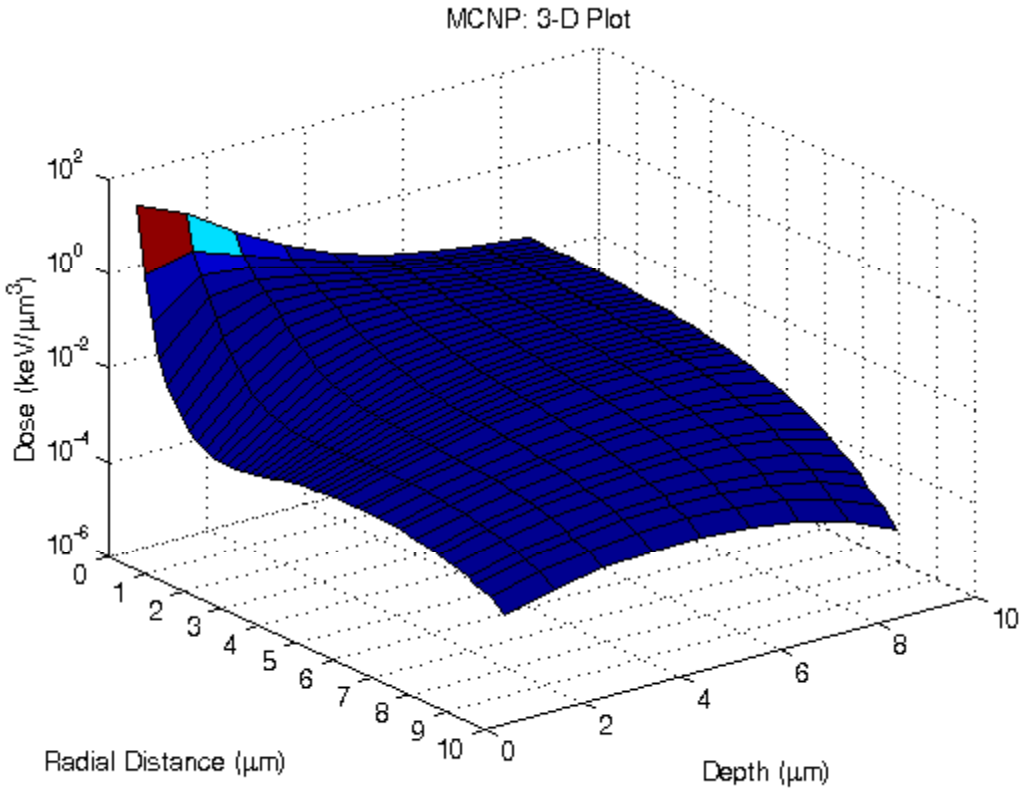

Figures 6.1 – 6.3: 3-D plots of dose distributions **D(r,x)** in **(keV/μm^3)** as function of radial distance (r) and of penetration (x) for each code: PENELOPE, MCNP, PITS.

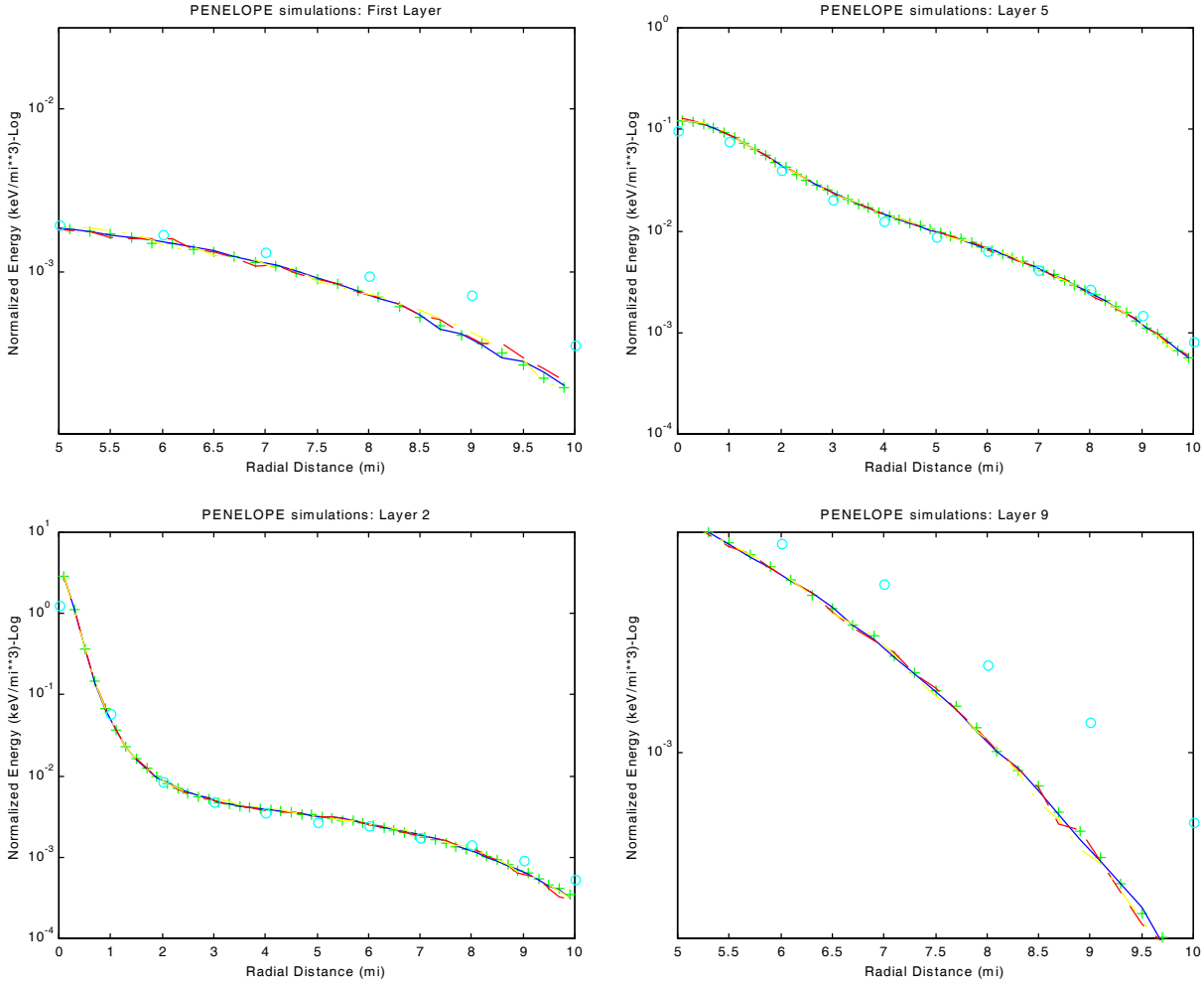

Figures 7.1 – 7.4: PENELOPE 2-D plots of radial dose distributions **D(r)** in **(keV/μm^3)**. Each figure represent a comparison of D(r) values computed with PENELOPE varying some parameters and zooming in a particular zone.

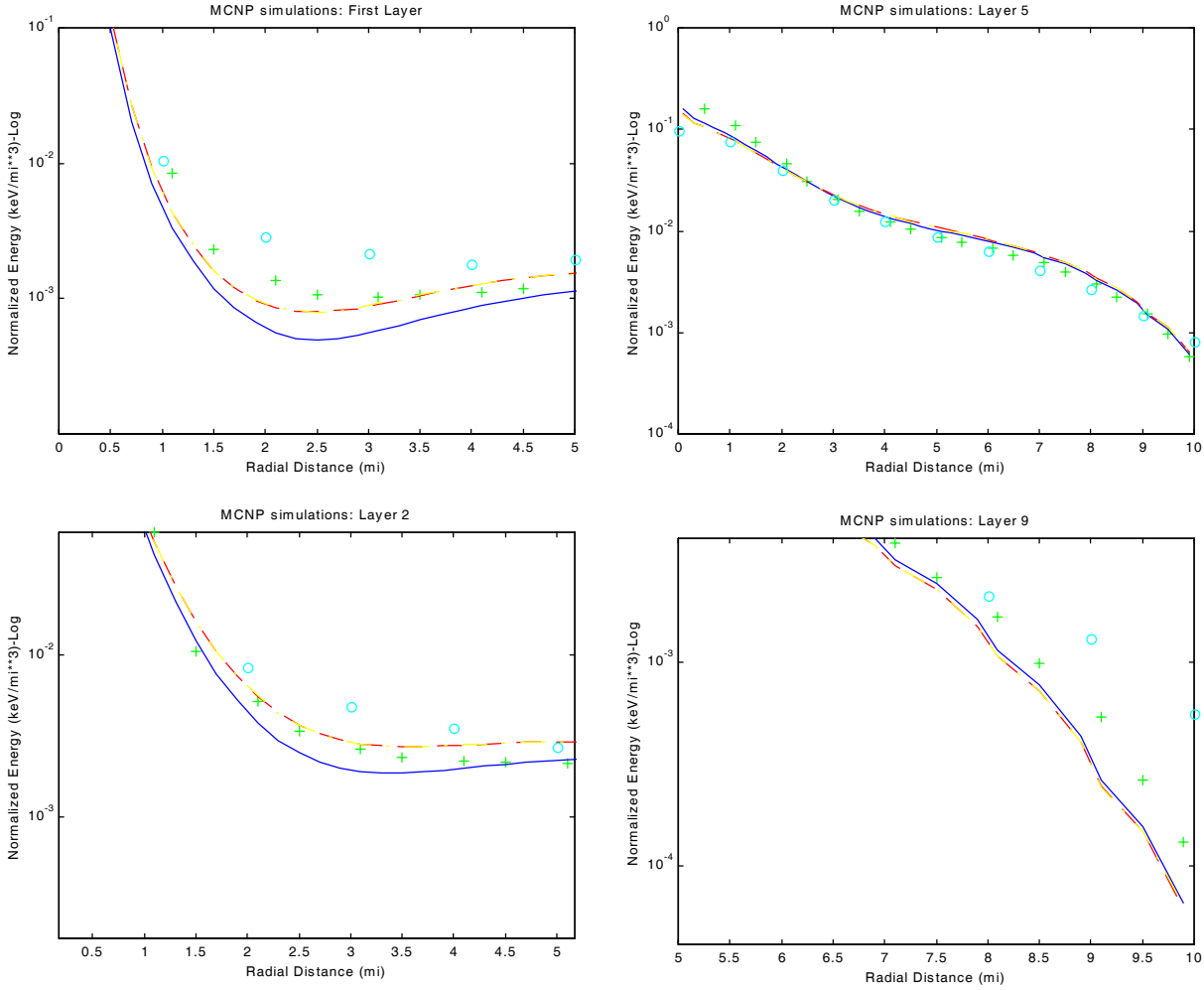

Figures 8.1 – 8.4: MCNP 2-D plots of radial dose distributions **D(r)** in **(keV/μm^3)**. Each figure represent a comparison of D(r) values computed with MCNP varying some parameters and zooming in a particular zone.